Systematics in the Pb^{208}-Th^{232}, Pb^{207}-U^{235}, and Pb^{206}-U^{238} Systems[1]

RUDOLF H. STEIGER AND G. J. WASSERBURG

Arms Laboratory of Geological Sciences
California Institute of Technology, Pasadena

In a study of cogenetic zircons it was found that the measured Pb^{208}/Th^{232} and Pb^{207}/U^{235} ratios formed a linear array in the corresponding coupled Pb-U-Th evolution diagram, which has an upper intersection on the concordia curve at the same time point as that determined by the Pb^{206}/U^{238}, Pb^{207}/U^{235} array. Although the U-Pb data lie in the accessible region for nonfractionating daughter loss, the Th-Pb results lie outside the corresponding region. The zircon concentrates analyzed were shown to be multiphase assemblages with variable U and Th contents and variable Th/U ratios, even within single crystals. The zircons contain local domains of high radioactivity which appear to be highly discordant. A relationship between discordance and the average concentration of U and Th in a sample is given. The degree of discordance increases with the concentration of U and Th and with the increasing Th/U ratio, causing preferential loss of Pb^{208} and the departure from the region accessible to a single phase without fractionation. The theoretical aspects of the ($r_{\lambda_{U^{238}}}$, $r_{\lambda_{Th^{232}}}$) diagram from the viewpoint of single-phase and multiphase assemblages are discussed, and it is shown that the variability of the Th/U ratio is of fundamental importance in understanding the evolution of the Th-U-Pb system. The existence of these systematics in nature may provide an additional independent dating system and a further means of studying transport from natural systems.

INTRODUCTION

In general, if a radioactive parent P with decay constant λ produces a stable daughter product D, the ratio of accumulated radiogenic daughter product to residual parent after a time t is defined to be r_λ. If there are a pair of such parent-daughter systems with decay constants λ, λ' it is possible to define the primary age of a system (i.e., when $r_\lambda = r_{\lambda'} = 0$) even when the natural systems are open [*Wetherill*, 1956, 1963; *Nicolaysen*, 1957; *Tilton*, 1960; *Wasserburg*, 1963] if certain rather general conditions obtain which generate a systematic relationship between possible sets of values of r_λ and $r_{\lambda'}$. The existence of such systematics is extremely important in age determinations and in understanding the mechanisms of transport of both parent and daughter products in geologic systems.

Systematic linear relationships in the coupled parent-daughter systems U^{238}–Pb^{206} and U^{235}–Pb^{207} are well documented, although the mechanisms of transport are still poorly understood.

Other systems may be useful in this connection, but it is most natural to expect the general conditions generating a regular relationship to obtain if the parents (and daughters) are isotopic species of a given element. The case of Th^{232}–Pb^{208} is in this manner distinct from the U^{235}–Pb^{207} and U^{238}–Pb^{206} systems and has therefore not been the subject of extensive investigation. From general considerations [*Wasserburg*, 1963], however, particularly if transport is dominated by nonfractionating diffusive daughter loss, a systematic behavior is to be expected for the $r_{\lambda_{U^{235}}}(=Pb^{207}/U^{235})$ and $r_{\lambda_{Th^{232}}}(=Pb^{208}/Th^{232})$ or $r_{\lambda_{U^{238}}}(=Pb^{206}/U^{238})$ and $r_{\lambda_{Th^{232}}}(=Pb^{208}/Th^{232})$ systems.

Until now very little attention has been paid to the Pb-U-Th systems, and only recently *Hart* [1966], in a review article, commented, 'Because there is only a single age, concordia type analysis cannot be used. . . .' However, *Ahrens* [1955] and C. Allègre[2] (personal communication) have discussed some constructions in the ($r_{\lambda_{U^{238}}}$, $r_{\lambda_{Th^{232}}}$) diagram and pointed out certain significant conclusions that may be drawn from such considerations. Some discussion of U-Th-Pb sys-

[1] California Institute of Technology Contribution 1421.

[2] While this manuscript was being prepared for publication a manuscript by C. Allègre entitled 'Discussion des âges U-Th-Pb discordants obtenus sur les mêmes échantillons: Concordia generalisée appliquée aux zircons' was received. This paper, in press in *Earth and Planetary Sciences Letters*, covers several of the topics included in the work presented here.

TABLE 1. Analytical Data of Cogenetic Zircons from the Sandia Granite, New Mexico

Sample	No.	Size, Magnetic Susceptibility	Sample Weight, grams	Concentrations,*† ppm U	Th	Pb^{206}	Th/U Ratio (Atomic)	Pb Atom Abundance* Relative to Pb^{206} = 100‡ 204	206	207	208
NM 5A§	β1	+325 mesh, non-magnetic	0.2502	418.2	182.1	84.24	0.447	0.3749	100	14.33	26.51
	β2	magnetic	0.1582	652.2	319.2	88.28	0.502	0.1051	100	10.52	18.03
NM 5B§	1	−120 + 150 mesh	0.1884	494.1	198.1	79.98	0.411	0.1183	100	10.56	‖
	2	−150 + 200 mesh	0.1050	484.0	233.3	78.78	0.494	0.1089	100	10.57	‖
	3	−150 + 230 mesh	0.3142	479.9	215.9	82.19	0.461	0.0812	100	10.18	16.41
	4	−230 mesh	0.2116	506.0	242.0	83.96	0.491	0.1035	100	10.48	17.74

* These data are corrected for blanks of 0.01 μg U, 0.03 μg Th, and 0.25 μg Pb (isotopic composition: 206/204, 18.6; 207/204, 15.9; 208/204, 38.6) which were applied to the 10% aliquot used for the U-Th and to the 30% aliquot used for the Pb determination.

† Estimated errors for concentrations: U, 1%; Th, 2%; Pb, 1%.

‡ Maximum uncertainty for ratios: 207/206, 0.4%; 208/206, 0.4%; observed 206/204 ratios vary from 500 to 900, except for sample β1 for which a ratio of 240 ± 2 was measured.

§ Samples A and B are pieces from a single large block of granite.

‖ Pb^{208} could not be determined because the Pb^{208} tracer was added to the total sample owing to the small sample size.

tems has also been given by *Nicolaysen* [1957] and *Aldrich et al.* [1965].

In the present report we give data from a study of a suite of zircons separated from a single block of the Sandia Mountain granite, for which determinations of the three Pb-U-Th ages were made (see Tables 1 and 2), and discuss some earlier data from the literature. The granite sample was obtained from a roadcut on Route 66 in the Tijeras Canyon, about 12.5 miles east of Albuquerque, New Mexico. The approximate sample location is 106°28′00″W and 35°03′50″N. A geological map of this area was published by *Kelley* [1963].

We will present the U-Th-Pb data and then discuss the behavior of cogenetic systems in terms of single-phase and multiphase systems. It will be shown that the observations cannot be explained by considering the average values of the U and Th contents of the system as if the system were a single phase. We will then attempt to prove that the heterogeneous distribution of these elements governs the systematics which are observed. The significance of the multiphase aspects will be emphasized in terms of a simple two-phase model. The point of this discussion is not simply to state the well-known fact that zircon separates are a mixture of inhomogeneous, impure crystals but to evaluate some important consequences which this conclusion has for our understanding of the discordance in natural systems.

TABLE 2. Ages of Cogenetic Zircons from the Sandia Granite, New Mexico

Sample	No.	Atom Ratios* Pb^{206}/U^{238}	Pb^{207}/U^{235}	Pb^{208}/Th^{232}	Pb^{207}/Pb^{206}	Apparent Ages† (in 10^6 Years) Pb^{206}/U^{238}	Pb^{207}/U^{235}	Pb^{208}/Th^{232}	Pb^{207}/Pb^{206}	Diffusion Ages (in 10^6 Years) $D = D_0$	$D(t) = D_1 t$
NM 5A	β1	0.2196	2.753	0 06684	0.09097	1290 ± 15	1360 ± 10	1295 ± 25	1470 ± 20	1510	1500
	β2	0 1547	1.931	0.04422	0.09056	935 ± 15	1105 ± 10	865 ± 20	1460 ± 20	1640	1580
NM 5B	1	0.1846	2.265		0.08904	1100 ± 15	1215 ± 10		1430 ± 20	1530	1490
	2	0.1860	2.319		0.09048	1110 ± 15	1235 ± 10		1460 ± 20	1560	1530
	3	0.1966	2.451	0.05765	0 09049	1170 ± 15	1275 ± 10	1125 ± 25	1455 ± 20	1530	1510
	4	0.1897	2.362	0 05456	0.09035	1130 ± 15	1250 ± 10	1065 ± 20	1455 ± 20	1540	1520

* Assumed isotopic composition for common Pb: 206/204, 16.9; 207/204, 15.50; 208/204, 36.50.

† Constants used: $\lambda_{U^{238}}$ 1.537 × 10^{-10} yr^{-1}, $\lambda_{U^{235}}$ 9.72 × 10^{-10} yr^{-1}, $\lambda_{Th^{232}}$ 4.99 × 10^{-11} yr^{-1}, U^{238}/U^{235} = 1/137.8.

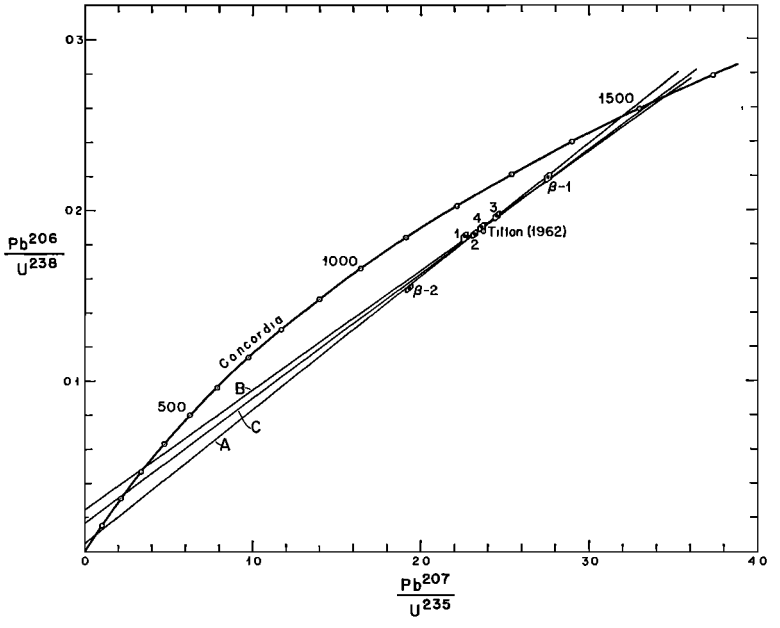

Fig. 1. Conventional ($r_{\lambda U^{235}}$, $r_{\lambda U^{238}}$) diagram showing the data points for cogenetic zircons from the Sandia granite, Albuquerque, New Mexico. A single determination from the previous work of *Tilton et al.* [1962] is also shown. Line A is a best-fit line to the data points. For an episodic model the intersections correspond to a primary age of 1470 m.y. and a disturbance of 60 m.y. ago. Line B is a best-fit straight line to the upper region of a continuous diffusion model $D = D_0$ (a constant) for 1530 m.y. Line C is a best-fit straight line to the upper region of a continuous diffusion model $D = D_1 t$ for 1510 m.y. The error boxes shown correspond to the estimated errors given in Table 2.

Uranium-Lead Relationships

We have investigated a series of cogenetic zircon samples from a single rock, following *Silver and Deutsch* [1961, 1963] and *Silver* [1962, 1963], in order to eliminate differential effects which may be present in rocks from different localities.

The zircon populations separated from this rock range from pink euhedral crystals with sharp terminations to somewhat rounded and less transparent crystals to opaque crystals. Six zircon fractions were isolated from the original sample and analyzed for Pb, U, and Th. The analytical data and corresponding ages are tabulated in Tables 1 and 2. The Pb-U data are presented in Figure 1 on a conventional ($r_{\lambda U^{235}}$, $r_{\lambda U^{238}}$) diagram. These data define a linear array which has an upper intercept on the concordia curve at approximately 1470 m.y. As shown by *Wasserburg* [1963], any diffusion-loss mechanism, whether continuous or episodic, will yield a linear array in the upper part of this diagram, and the intersection with the concordia curve is the primary age of the system. Considering all analytical uncertainties, the possible straight-line fits to these data would indicate that the primary age lies between 1450 and 1510 m.y., the most reasonable value being 1470 m.y. From the sample descriptions given earlier, it is evident that one may not assume that the sample population is all cogenetic. However, the data shown here do not indicate any obvious difference in primary ages which has persisted through the event of about 1470 m.y. ago. We will therefore ignore the effects of primary age variations in the zircon population and attempt to discuss some of the possible means of generating the discordant relationship seen.

Following the treatment of *Wetherill* [1956], it is clear from Figure 1, line A, that these data are compatible with episodic loss about 60 m.y. ago. Evidence has already been presented by *Wasserburg et al.* [1965] on the presence of anomalous Sr in accessory minerals in this rock, indicating some element redistribution. The times at which this may have occurred are not

TABLE 3. Degree of Discordance and Content of Radioactive Elements

Sample	No.	$f = \frac{Pb^{206}/U^{238}}{\exp(\lambda_{U^{238}}t) - 1}$	U + eq. Th,* ppm
NM 5	$\beta 1$	0.866	460
	$\beta 2$	0.610	725
	1	0.728	540
	2	0.734	538
	3	0.776	529
	4	0.748	561

* U + equivalent Th.

clear at present, however, because the Sandia Mountains are part of the Basin and Range province, there is evidence that tectonic disturbances have been present well into Tertiary time.

Diffusion trajectories for the continuous diffusion model with constant D [*Tilton*, 1960] were calculated for various primary ages, and it was found that a 1530-m.y. curve gave the best fit to the data points. Line B in Figure 1 is a best-fit straight line to the upper (linear) region of this 1530-m.y. trajectory. Though this line passes through all of the upper five experimental data points, it lies far above the sixth and lowest data point by approximately a factor of 6 outside analytical error. Using the continuous radiation damage diffusion model proposed by *Wasserburg* [1963], we obtained a best-fit straight line (Figure 1, line C) in a way similar to that described above. This line has an intercept of 1510 m.y. and passes through all the data points except the lowest one. It lies above the lowest point by approximately three times the analytical error. Of the two continuous diffusion mechanisms that have been mentioned, it would thus appear that the radiation damage diffusion model is more compatible with these experimental data than the constant D model. Because of the curvature in the continuous diffusion curves, the question of whether episodic or continuous diffusion has taken place can be clarified by obtaining data on more highly discordant samples. This locality does not appear optimal for the clarification of the problem because of the closeness of fit of both models to the data and because a mixture of both effects, namely recent diffusion loss and continuous diffusion loss with radiation damage, would still give an essentially linear array for this case.

The degree of discordance of the various zircon fractions analyzed is seen from Table 3 to be strongly related to the total concentration of U and Th. This supports the findings of *Silver and Deutsch* [1963] and indicates that radiation damage must be a primary cause of the diffusive loss of Pb, whether by continuous diffusion or by episodic diffusion losses.

It was proposed for diffusion-loss mechanisms related to radiation damage [*Wasserburg*, 1963] that the diffusion coefficient is proportional to the integrated radiation damage and hence approximately proportional to the total U and equivalent Th concentrations. Assuming that the characteristic diffusion distance a is the same for a suite of samples and that no parent loss occurs, it is possible to calculate the diffusion coefficients of different samples if one diffusion coefficient is known. For the models of episodic

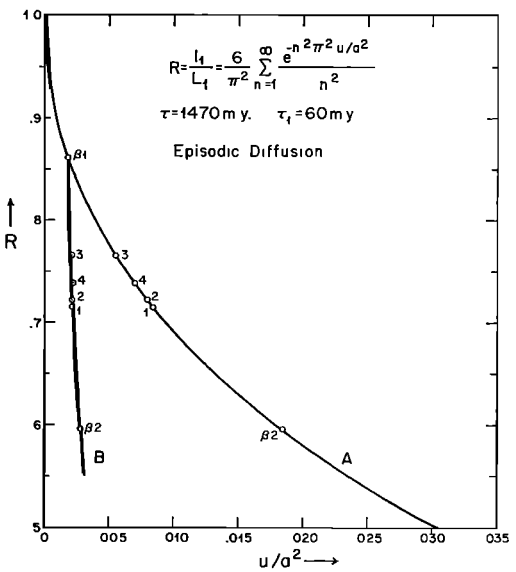

Fig. 2*a*. Graph of $R = \{[\exp(\lambda_{U^{238}}t_1) - 1]\}/[\exp(\lambda_{U^{238}}t) - \exp(\lambda_{U^{238}}t_1)]$ versus u/a^2 for the episodic diffusion model $D(t) = u\delta(t - t_1)$. The experimental points are plotted on curve A at the values of u/a^2 necessary to obtain the observed R values. Curve B is drawn through the points calculated from the experimental data with the assumptions that a^2 is constant and that u/a^2 is proportional to the α-particle flux (i.e., $(u/a^2)_{\beta 2} = (u/a^2)_{\beta 1}$(U + equivalent Th)$_{\beta 2}$/(U + equivalent Th)$_{\beta 1}$. The point for $\beta 1$ is assumed to lie on the theoretical curve.

diffusion loss [$D(t) = u\delta(t - t_1)$], constant diffusion coefficient [D_0], and diffusion coefficient proportional to time [D_1t], it follows that u, D_0, and D_1 should be proportional to the U plus equivalent Th concentrations. Figure 2 shows comparisons of degree of discordance of $r_{\lambda U^{238}}$ for various models as a function of the corresponding diffusion parameter. The gross discrepancies between the theoretical curves (A and A′) and the experimental curves B and B′ should be noted. The experimental points are shown in each figure, the diffusion parameters corresponding to the experimentally determined degree of discordance. Assuming the value of the diffusion parameter calculated for sample $\beta 1$ and the proportionality relationship referred to above, the diffusion parameters of the other samples were calculated and are shown by the curves marked B in Figure 2. It is evident that the diffusion parameters u/a^2, D_0, and D_1 increase far more rapidly with an increase in the average concentration of the radioactive elements than the proportionality relationship suggested by *Wasserburg* [1963]. It follows that some of the fundamental assumptions are in error in all these models. One possibility is that the diffusion length is inversely correlated with U and Th concentration. In the above calculation each sample fraction analyzed is assumed to represent a single phase, not a mixture of phases having different concentrations of radioactive elements. We will discuss the multiphase case later in this work.

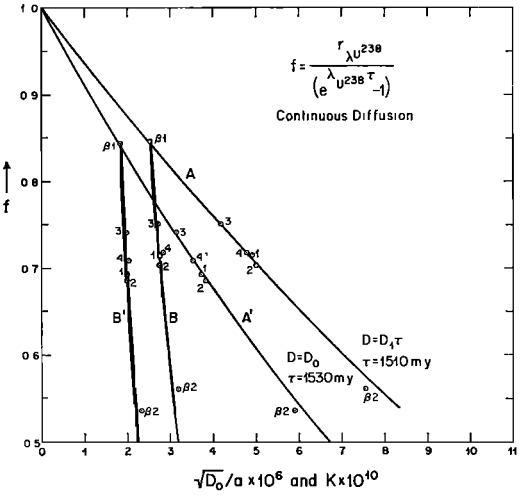

Fig. 2*b*. A graph of $f = r_{\lambda U^{238}}/(e^{\lambda U^{238} t} - 1)$ versus the diffusion parameters $K(K = \pi\sqrt{2D_1}/a)$ and $\sqrt{D_0}/a$ for two continuous diffusion models. Curve A corresponds to $D(t) = D_1t$ and curve A′ corresponds to $D(t) = D_0$, a constant. The curves B and B′ are drawn through the data points assuming that $D(t)/a^2$ is proportional to the U + eq. Th concentrations for the respective model. The point for $\beta 1$ is assumed to lie on the corresponding theoretical curve.

Thorium-Lead Relationships

Figures 3 and 4, respectively, show the experimental results plotted in a ($r_{\lambda U^{238}}$, $r_{\lambda Th^{232}}$) and a ($r_{\lambda U^{238}}$, $r_{\lambda Th^{232}}$) diagram. The general form of the concordia curve in the ($r_{\lambda U^{238}}$, $r_{\lambda Th^{232}}$) diagram is similar to that in the ($r_{\lambda U^{238}}$, $r_{\lambda U^{238}}$) diagram, since the high degree of curvature is due to the relatively short U^{235} half-life. The concordia curve in the ($r_{\lambda U^{238}}$, $r_{\lambda Th^{232}}$) diagram is very straight because both half-lives are very long and the times involved are much shorter than the half-lives. It can be seen by inspection that in both diagrams the experimental points form a linear array and that the sequence of discordance for these points corresponds to that found in the ($r_{\lambda U^{238}}$, $r_{\lambda U^{238}}$) diagram. A best fit to these points on a ($r_{\lambda U^{238}}$, $r_{\lambda Th^{232}}$) diagram is compatible with an intercept of 1470 m.y. on the concordia curve as was obtained for the ($r_{\lambda U^{238}}$, $r_{\lambda U^{238}}$) diagram. The experimental error for the point β-1 is rather large, because of a sizeable correction for common Pb with an uncertain Pb^{208}/Pb^{204} ratio. A best fit line for the ($r_{\lambda U^{238}}$, $r_{\lambda Th^{232}}$) diagram gives an intersection on concordia of approximately 1470 m.y. These data clearly demonstrate that it is possible to obtain linear arrays for the Th-Pb, U-Pb system, that their intercept on the concordia curve is compatible with that obtained from the ($r_{\lambda U^{238}}$, $r_{\lambda U^{238}}$) diagram, and that the degree of discordance in the Th ages follows that observed for the U ages, being a monotonically increasing function of the integrated radiation damage.

There exists some uncertainty with regard to the half-life of Th^{232}, as in the case of U^{235}. We have therefore indicated two concordia curves in Figures 3 and 4 corresponding to Th decay constants of 4.99 and 4.88 $\times$ 10^{-11} yr^{-1}. The upper curve is for the decay constant determined by *Kovarik and Adams* [1938], and the lower one is for the value reported by *Senftle et al.* [1956]. Assuming that the upper intersection of a line (drawn through a linear array) with the concordia

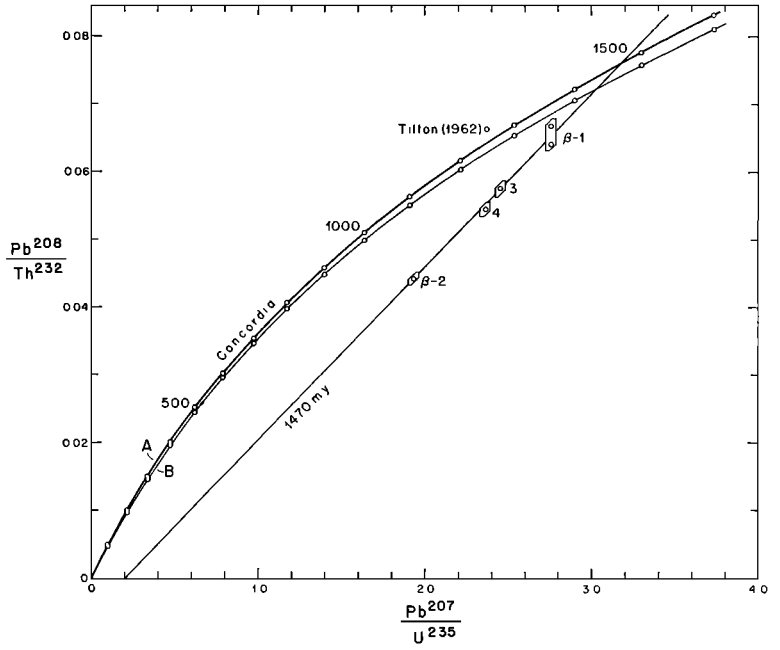

Fig. 3. An ($r_{\lambda_{U^{235}}}$, $r_{\lambda_{Th^{232}}}$) diagram showing the linear array formed by the data points for cogenetic zircons from the Sandia granite. Sample $\beta 1$ is corrected for a sizeable amount of common Pb with assumed Pb^{208}/Pb^{204} ratios of 36.5 and 38.0, as indicated by the two points. A single determination from the previous work of *Tilton et al.* [1962] is shown. The concordia curve for this diagram is given for $\lambda_{Th^{232}} = 4.99 \times 10^{-11}$ yr^{-1} (curve A) in heavy line and for $\lambda_{Th^{232}} = 4.88 \times 10^{-11}$ yr^{-1} (curve B). Note that the best-fit line intersects the abcissa to the right of the origin.

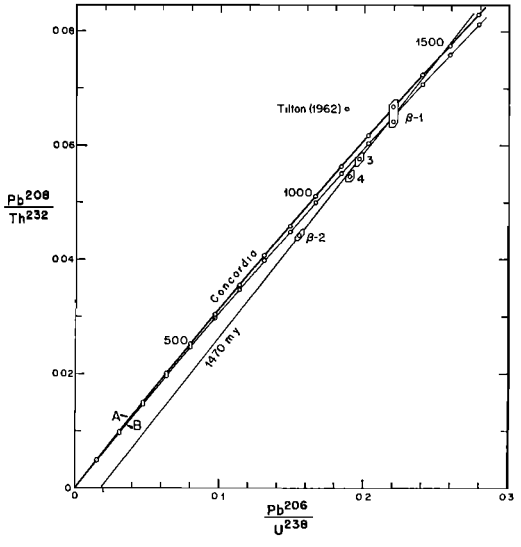

Fig. 4. An ($r_{\lambda_{U^{235}}}$, $r_{\lambda_{Th^{232}}}$) diagram. Concordia curves A and B for constants are as in Figure 3.

curve corresponds to the time of a primary event, we can use this diagram to show the internal compatibility of the decay constants for the various pairs of decay schemes. It would appear in both cases that the experimental data, though very limited, suggest that the intersection with the upper curve (A) for $\lambda_{Th^{232}} = 4.99 \times 10^{-11}$ yr^{-1} is much closer to that obtained in Figure 1, and it seems more reasonable at present to continue using this decay constant rather than the value given by Senftle et al. In a more refined series of measurements it should be possible to provide a much stronger comparison of this sort and cast some light on the values of the decay constants in terms of an internally consistent set.

Theoretical Considerations

One-phase system. The general theory of the ($r_{\lambda_{U^{235}}}$, $r_{\lambda_{Th^{232}}}$) diagram is identical with that shown by previous workers [*Wetherill*, 1956; *Tilton*, 1960; *Wasserburg*, 1963] and may be considered in terms of a general (r_λ, $r_{\lambda'}$) diagram. For simplicity we will first confine our discussion

to daughter loss from a single phase which does not fractionate daughter isotopes or parent elements. In the event that the effects of discordance are caused by episodic transport loss, the upper and lower intersections with the concordia curve will correspond to the primary and secondary events, respectively. For different pairs of decay schemes, the intersections on all of the corresponding concordia curves will give the same ages.

If continuous nonfractionating diffusion were to take place, the diffusion trajectories would follow the general relationships described by *Wasserburg* [1963]. The lower intercepts for the asymptotic lines (tangents to the discordia curves) passing through concordia at various primary ages have been calculated for the ($r_{\lambda U^{238}}$, $r_{\lambda Th^{232}}$) and ($r_{\lambda U^{238}}$, $r_{\lambda Th^{232}}$) diagrams for the constant D and the radiation damage model cases, assuming no fractionation in Pb transport. If nonfractionating diffusive transport took place, we would expect to observe a regular relationship between the upper and lower intercepts on the concordia curves on all three diagrams for best-fit lines through an array of experimental data, these values all being predicted theoretically from the particular diffusion model used.

One important conclusion which follows from the asymptotic treatment for all three (r_λ, $r_{\lambda'}$) diagrams referred to above is that the times corresponding to the lower intersections with concordia are to first order all equal for a given age. The approximate coincidence of the lower and upper time intersections for these three diagrams does not aid in distinguishing episodic and continuous diffusion processes unless the time of the episode is distinct from that of the lower intersections. The numerical results for both the asymptotic and the exact solution to both continuous diffusion models have been calculated and may be obtained from the authors.

As shown by *Wasserburg* [1963, Figure 9], the experimental data points in an ($r_{\lambda U^{238}}$, $r_{\lambda U^{235}}$) plane must lie in an accessible region which is defined by the particular loss mechanism under consideration. This result holds more generally for a one-phase system. For systems subjected to pure daughter loss, it was shown that the accessible region lies between the concordia curve and the straight line from the origin to the point on the concordia curve corresponding to the time of the primary event. This type of behavior has been typically found for most ($r_{\lambda U^{238}}$, $r_{\lambda U^{235}}$) diagrams for zircons and other minerals. A very fundamental difference, however, appears for the experimental results presented here for the case of the ($r_{\lambda U^{238}}$, $r_{\lambda Th^{232}}$) and ($r_{\lambda U^{238}}$, $r_{\lambda Th^{232}}$) diagrams. This is particularly true in Figure 3, where it can be seen that the extrapolated line through these points lies to the right of the origin. It therefore follows that for a single-phase system this type of linear array is not explainable in terms of a nonfractionating diffusion loss mechanism, either continuous or episodic in character.

We are therefore led to consider the case of episodic loss with fractionation. The results presented by *Wetherill* [1956] may be generalized to the following form to include fractionation.

$$\begin{aligned} r_\lambda(t) &= R[e^{\lambda t} - e^{\lambda t_1}] + e^{\lambda t_1} - 1 \\ r_{\lambda'}(t) &= R'[e^{\lambda' t} - e^{\lambda' t_1}] + e^{\lambda' t_1} - 1 \end{aligned} \qquad t > t_1 \qquad (1)$$

where $R = e^{a_1}$ and $R' = e^{a'_1}$. R is the ratio of daughter to parent immediately after the episode at time t_1 to the value just before the episode. The notation is that used by *Wetherill* [1956].

We will first show that it is unreasonable to take R' proportional to R and then indicate a more valid dependence of R' on R for the case of fractionation.

If one assumes that $R'/R = K$ (a positive constant) for all possible values of R (0 to ∞), it follows that

$$\frac{r_{\lambda'}(t) - e^{\lambda' t_1} + 1}{r_\lambda(t) - e^{\lambda t_1} + 1} = K\left[\frac{e^{\lambda' t} - e^{\lambda' t_1}}{e^{\lambda t} - e^{\lambda t_1}}\right]$$

The trajectory of (r_λ, $r_{\lambda'}$) for the parameter R is then a straight-line segment starting from the point on concordia corresponding to t_1 and passing through the concordia curve at some time t^+ (which is not of physical significance). If the loss of daughter (or gain of parent) in the λ' daughter-parent pair is preferential, K is less than unity and $t^+ > t$. This model is not very reasonable physically because it requires a decrease in $r_{\lambda'}$ for the case when r_λ is concordant.

Consideration of episodic diffusion loss seems to indicate a more plausible functional relationship between R' and R. If the diffusion coefficients of daughter and parent are $D(t) = u\,\delta(t - t_1)$ and $D^*(t) = u^*\,\delta(t - t_1)$ (see Appendix A), we obtain

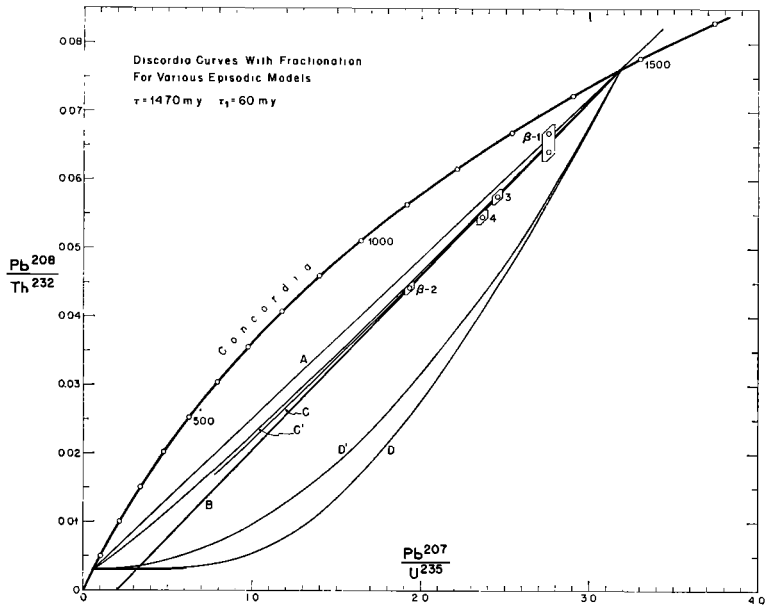

Fig. 5. An $(r_{\lambda_{U^{238}}}, r_{\lambda_{Th^{232}}})$ diagram showing various trajectories for one-phase systems subjected to episodic loss. Line A corresponds to a model with no fractionation; line B is the best fit to the data points, its slope is 1.091 times slope of line A; curves C and C' are for diffusion model losses with the fractionation $(u/a^2)_{Pb^{206}} = (1.091)^2 (u/a^2)_{Pb^{207}}$ and a homogeneous system model with the fractionation $R' = R^{1.091}$, respectively; curves D and D' are for $(u/a^2)_{Pb^{206}} = (2)^2(u/a^2)_{Pb^{207}}$ and $R' = e^{2a_1} = R^2$, respectively.

$$R = \frac{g(u/a^2)}{g(u^*/a^2)} = \frac{\sum_{n=1}^{\infty} \frac{1}{n^2} e^{-n^2\pi^2 u/a^2}}{\sum_{m=1}^{\infty} \frac{1}{m^2} e^{-m^2\pi^2 u^*/a^2}}$$

If we consider the diffusion coefficient of the λ' daughter to be greater than that of the λ daughter by a positive factor of k, then $R' = g(ku/a^2)/g(u^*/a^2)$. It follows that if the parametric form given by *Wetherill* [1956] is used it is physically reasonable to take $a'_1 = ka_1$ (i.e., $R' = (R)^k$), which gives, upon substitution in (1),

$$\frac{r_{\lambda'}(t) - e^{\lambda' t_1} + 1}{r_\lambda(t) - e^{\lambda t_1} + 1} = e^{(k-1)a_1}\left[\frac{e^{\lambda' t} - e^{\lambda' t_1}}{e^{\lambda t} - e^{\lambda t_1}}\right]$$

As a_1 ranges from $-\infty$ to $+\infty$, $(r_\lambda, r_{\lambda'})$ describe a *curve* starting on the concordia curve at time t_1 with zero slope and passing through the concordia curve at time t with a slope equal to k times the slope of the straight-line chord from t_1 to t. A graph of the preceding case is given in Figure 5.

For continuous diffusion loss of daughter product, the trajectory $(r_\lambda, r_{\lambda'})$ is approximately linear in a neighborhood about the concordia. The equations are given by *Wasserburg* [1963, p. 4841, eq. 2). Assuming the diffusion coefficient of the λ' daughter to be a constant k times that of the λ daughter, it follows that the equation of the line is

$$\frac{r_{\lambda'} - e^{\lambda' t} + 1}{r_\lambda - e^{\lambda t} + 1} = \sqrt{k}\,\frac{\lambda' e^{\lambda' t}\int_0^t e^{-\lambda'\eta}[T(t) - T(\eta)]^{1/2}\,d\eta}{\lambda e^{\lambda t}\int_0^t e^{-\lambda\xi}[T(t) - T(\xi)]^{1/2}\,d\xi} = \frac{dr_{\lambda'}}{dr_\lambda} = \text{a constant} \qquad (2)$$

That is, the slope is changed by the ratio of the square roots of the diffusion coefficients $\sqrt{k} = (D'/D)^{1/2}$. This result applies to both the continuous and episodic diffusion models.

Two-phase system. The behavior of Th-U-Pb systems is intrinsically more complicated for open systems than the U-Pb systems because of the fact that the Th/U ratio is not constant, whereas the U^{235}/U^{238} ratio is constant in natural

terrestrial materials. This has very marked effects for even the simplest type of deviation from closed-system behavior, since most of the mineral separates analyzed for age determination are heterogeneous. Let us consider a system composed of two phases α and β. By a phase we mean a mass of chemically and physically homogeneous matter. Two domains of the same crystal but with different chemical compositions are to be considered as separate phases. The ratios of daughter to parent in this total system can be written in terms of the intensive properties $r_\lambda{}^\alpha$ of the two phases and the relative proportions of Pb, U, and Th which they contribute. For the total system we have

$$r_{\lambda_{Th^{232}}} = \frac{Pb_\alpha{}^{208} + Pb_\beta{}^{208}}{Th_\alpha{}^{232} + Th_\beta{}^{232}} = y^\alpha r^\alpha{}_{\lambda_{Th^{232}}} + y^\beta r^\beta{}_{\lambda_{Th^{232}}}$$

$$r_{\lambda_{U^{235}}} = \frac{Pb_\alpha{}^{207} + Pb_\beta{}^{207}}{U_\alpha{}^{235} + U_\beta{}^{235}} = x^\alpha r^\alpha{}_{\lambda_{U^{235}}} + x^\beta r^\beta{}_{\lambda_{U^{235}}} \qquad (3)$$

$$r_{\lambda_{U^{238}}} = \frac{Pb_\alpha{}^{206} + Pb_\beta{}^{206}}{U_\alpha{}^{238} + U_\beta{}^{238}} = x^\alpha r^\alpha{}_{\lambda_{U^{238}}} + x^\beta r^\beta{}_{\lambda_{U^{238}}}$$

The symbols of the nuclides represent the total number of atoms in each phase. Here $r_\lambda{}^\alpha$ and $r_\lambda{}^\beta$ are the daughter-to-parent ratios for phases α and β and x^α, x^β, y^α, and y^β are the mole fractions of the total U or Th which are in each phase, i.e., $x^\alpha + x^\beta = 1$, $y^\alpha + y^\beta = 1$, and

$$x^\alpha = U_\alpha{}^{238}/(U_\alpha{}^{238} + U_\beta{}^{238})$$
$$y^\alpha = Th_\alpha{}^{232}/(Th_\alpha{}^{232} + Th_\beta{}^{232}) \qquad (4)$$

The behavior of such a system is illustrated in Figure 6. The trajectories of ($r_{\lambda_{U^{238}}}$, $r_{\lambda_{Th^{232}}}$) are plotted for end members *a*, *b*, and *c*. Curves A and B are for $(Th/U)_a/(Th/U)_b = 12$ and 1/12, respectively. If the more discordant phase has a higher Th/U ratio, the mixtures lie beneath the line *ab*. If it has a lower Th/U ratio, the mixtures lie above *ab*. Curve C is for the case $(Th/U)_a/(Th/U)_b = 2$. Even a small enrichment causes marked departures from the line *ab*.

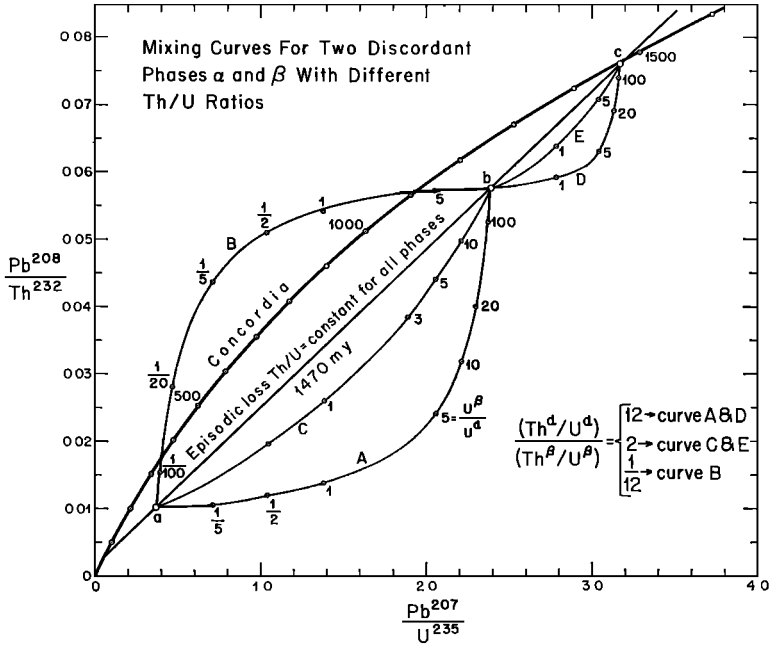

Fig. 6. An ($r_{\lambda_{U^{238}}}$, $r_{\lambda_{Th^{232}}}$) diagram showing trajectories for various mixtures between two phases of varying discordance and different relative Th/U ratios, i.e., different distribution coefficients. Phases *a* and *b* are 90 and 25% discordant, respectively; phase *c* is concordant. The numbers on each curve indicate the particular U^β/U^α ratio for each point. Here the superscripts α and β stand for the more discordant and less discordant phases, respectively.

Curves D and E are for discordant phase b and concordant phase c, if the discordant phase b is assumed to have the higher Th/U ratio. It is clear from these simple examples that discordant multiphase Pb-U-Th systems are intrinsically complex.

Following *Wetherill* [1956], let us suppose for simplicity that a system of primary age t suffered an episodic disturbance a time t_1 years ago. Let

$$R^{\alpha}{}_{Th^{232}} \equiv (r^{\alpha}{}_{\lambda_{Th^{232}}})_A/(r^{\alpha}{}_{\lambda_{Th^{232}}})_B$$

$$R^{\beta}{}_{Th^{232}} \equiv (r^{\beta}{}_{\lambda_{Th^{232}}})_A/(r^{\beta}{}_{\lambda_{Th^{232}}})_B$$

where A and B refer to the values immediately after and before the disturbance, respectively. Then if the system was closed except during the episode and if the isotopes of U and Pb^{206} and Pb^{207} are not fractionated, we obtain after substitution in (3)

$$\begin{aligned} r_{\lambda_{Th^{232}}}(t) &= [y_A{}^{\alpha}(R^{\alpha}{}_{Th^{232}} - R^{\beta}{}_{Th^{232}}) + R^{\beta}{}_{Th^{232}}] \\ &\quad \cdot[\exp(\lambda_{Th^{232}}t) - \exp(\lambda_{Th^{232}}t_1)] \\ &\quad + \exp(\lambda_{Th^{232}}t_1) - 1 \\ r_{\lambda_{U^{238}}}(t) &= [x_A{}^{\alpha}(R^{\alpha}{}_{U^{238}} - R^{\beta}{}_{U^{238}}) + R^{\beta}{}_{U^{238}}] \\ &\quad \cdot[\exp(\lambda_{U^{238}}t) - \exp(\lambda_{U^{238}}t_1)] \\ &\quad + \exp(\lambda_{U^{238}}t_1) - 1 \qquad (5) \\ r_{\lambda_{U^{235}}}(t) &= [x_A{}^{\alpha}(R^{\alpha}{}_{U^{235}} - R^{\beta}{}_{U^{235}}) + R^{\beta}{}_{U^{235}}] \\ &\quad \cdot[\exp(\lambda_{U^{235}}t) - \exp(\lambda_{U^{235}}t_1)] \\ &\quad + \exp(\lambda_{U^{235}}t_1) - 1 \end{aligned}$$

Here $x_A{}^{\alpha}$ and $y_A{}^{\alpha}$ refer to the mole fractions immediately *after* the disturbance.

The well-known result follows that the pair of values ($r_{\lambda_{U^{238}}}$, $r_{\lambda_{U^{235}}}$) for all values of $R^{\alpha}{}_{U^{238}}$, $R^{\beta}{}_{U^{238}}$, and x^{α} lie on a straight line passing through the points t_1 and t on the concordia curve. On the other hand, the pairs of values ($r_{\lambda_{U^{238}}}$, $r_{\lambda_{Th^{232}}}$) do not lie on a straight line even if there is no fractionation of Th and U or of the Pb isotopes (i.e., $R^{\alpha}{}_{Th^{232}} = R^{\alpha}{}_{U^{238}}$, $R^{\beta}{}_{Th^{232}} = R^{\beta}{}_{U^{238}}$). Under this constraint we drop the subscript on the variable R^{α} in (5) and obtain

$$\begin{aligned} r_{\lambda_{Th^{232}}}(t) &= [y_A{}^{\alpha}\{R^{\alpha} - R^{\beta}\} + R^{\beta}] \\ &\quad \cdot[\exp(\lambda_{Th^{232}}t) - \exp(\lambda_{Th^{232}}t_1)] \\ &\quad + \exp(\lambda_{Th^{232}}t_1) - 1 \\ r_{\lambda_{U^{238}}}(t) &= [x_A{}^{\alpha}\{R^{\alpha} - R^{\beta}\} + R^{\beta}] \\ &\quad \cdot[\exp(\lambda_{U^{238}}t) - \exp(\lambda_{U^{238}}t_1)] \\ &\quad + \exp(\lambda_{U^{238}}t_1) - 1 \end{aligned} \qquad (6)$$

$$\frac{r_{\lambda_{Th^{232}}} - \exp(\lambda_{Th^{232}}t) + 1}{r_{\lambda_{U^{238}}} - \exp(\lambda_{U^{238}}t) + 1} = \frac{[\exp(\lambda_{Th^{232}}t) - \exp(\lambda_{Th^{232}}t_1)][y_A{}^{\alpha}\{R^{\alpha} - R^{\beta}\} + R^{\beta} - 1]}{[\exp(\lambda_{U^{238}}t) - \exp(\lambda_{U^{238}}t_1)][x_A{}^{\alpha}\{R^{\alpha} - R^{\beta}\} + R^{\beta} - 1]}$$

For the case of only one phase (say α), or if $y^{\alpha} = x^{\alpha}$ (i.e., the Th/U ratio is the same in both phases) or if $R^{\alpha} = R^{\beta}$, the equations 6 reduce to the equations 1 given by *Wetherill* [1956]. It follows that a one-phase system or a set of separate one-phase systems which have suffered loss without fractionation lies on a chord in the ($r_{\lambda_{U^{238}}}$, $r_{\lambda_{Th^{232}}}$) diagram which intersects the concordia curve at points corresponding to t_1 and t. A mixture of phases will, however, not lie on this line. The coefficient on the right-hand side must be treated with caution because the variables $y_A{}^{\alpha}$, $x_A{}^{\alpha}$, R^{α}, and R^{β} are interrelated,

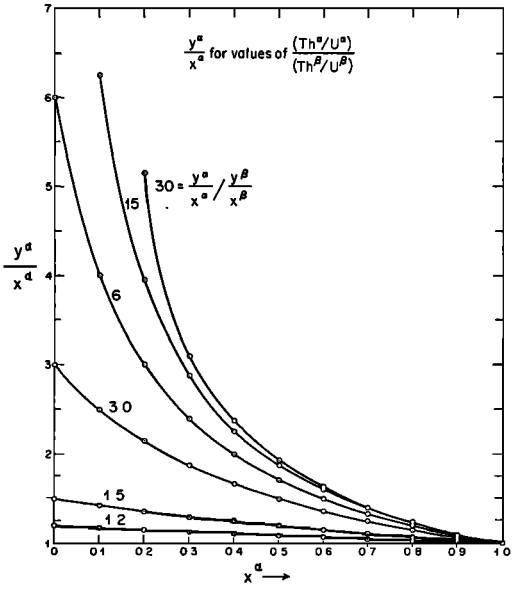

Fig. 7. The mole fraction of the total Th in the sample which is present in phase α divided by the mole fraction of the total U in the sample present in phase $\alpha[y^{\alpha}/x^{\alpha} = (Th^{\alpha}/Th^{\alpha} + Th^{\beta})/(U^{\alpha}/U^{\alpha} + U^{\beta})]$ versus x^{α}, the mole fraction of the total U present in phase $\alpha[x^{\alpha} = U^{\alpha}/(U^{\alpha} + U^{\beta})]$.

depending on the losses. For this reason it is convenient to define some parameters to describe the physical processes that we envision. Let l_j^α be the fraction of the daughter isotope of parent j lost from phase α and L_j^α be the fraction of parent isotope lost from phase α:

$$l_j^\alpha \equiv \frac{(\mathrm{Pb}_\alpha{}^j)_{\text{before}} - (\mathrm{Pb}_\alpha{}^j)_{\text{after}}}{(\mathrm{Pb}_\alpha{}^j)_{\text{before}}}$$

$$L_j^\alpha \equiv \frac{(N_\alpha{}^j)_{\text{before}} - (N_\alpha{}^j)_{\text{after}}}{(N_\alpha{}^j)_{\text{before}}}$$

where N_j^α is the total number of parent j in phase α. Then, designating the undisturbed system by B (before), we find that

For this elementary case, where both phases were concordant before the disturbance, it follows that they move off of the line t_1t unless the system consists of only one phase, or $y^\alpha = x^\alpha$. This means that even though each phase moves along the line t_1t the total system departs from this line. This departure is a direct reflection of the ratio

$$y_B{}^\alpha / x_B{}^\alpha = \frac{\mathrm{Th}_\alpha{}^{232}}{\mathrm{U}_\alpha{}^{238}} \Big/ \left(\frac{\mathrm{Th}_\alpha{}^{232} + \mathrm{Th}_\beta{}^{232}}{\mathrm{U}_\alpha{}^{238} + \mathrm{U}_\beta{}^{238}}\right).$$

This is the enrichment factor of the Th/U value for phase α over that for the total system. The function $y_B{}^\alpha/x_B{}^\alpha$ ranges from the distribution coefficient $(\mathrm{Th}_\alpha{}^{232}/\mathrm{U}_\alpha{}^{238})/(\mathrm{Th}_\beta{}^{232}/\mathrm{U}_\beta{}^{238})$ for $x_B{}^\alpha =$ 0 to 1 for $x_B{}^\alpha = 1$ (Figure 7). If the distribution coefficient is significantly greater than unity, then, in order for $y_B{}^\alpha/x_B{}^\alpha$ to be near unity, $x_B{}^\alpha$ must be around 1 (i.e., almost all of the U and Th must be in phase α). It may be noted that for a distribution coefficient of 1.333, x^α must be greater than 0.63 in order for y^α/x^α to be less than 1.10.

$$r_{\lambda_{\mathrm{Th}^{232}}}(t) = \frac{[(1 - l^\alpha{}_{\mathrm{Pb}^{208}})y_B{}^\alpha + (1 - l^\beta{}_{\mathrm{Pb}^{208}})y_B{}^\beta][\exp(\lambda_{\mathrm{Th}^{232}}t) - \exp(\lambda_{\mathrm{Th}^{232}}t_1)]}{[y_B{}^\alpha(1 - L^\alpha{}_{\mathrm{Th}^{232}}) + y_B{}^\beta(1 - L^\beta{}_{\mathrm{Th}^{232}})]} + \exp(\lambda_{\mathrm{Th}^{232}}t_1) - 1$$

$$r_{\lambda_{\mathrm{U}^{235}}}(t) = \frac{[(1 - l^\alpha{}_{\mathrm{Pb}^{207}})x_\beta{}^\alpha + (1 - l^\beta{}_{\mathrm{Pb}^{207}})x_B{}^\beta][\exp(\lambda_{\mathrm{U}^{235}}t) - \exp(\lambda_{\mathrm{U}^{235}}t_1)]}{[x_B{}^\alpha(1 - L^\alpha{}_{\mathrm{U}^{235}}) + x_B{}^\beta(1 - L^\beta{}_{\mathrm{U}^{235}})]} + \exp(\lambda_{\mathrm{U}^{235}}t_1) - 1 \qquad (7)$$

In general, for the single-episode model the minimum values of $r_{\lambda_{\mathrm{U}^{235}}}$ and $r_{\lambda_{\mathrm{Th}^{232}}}$ are $\exp(\lambda_{\mathrm{U}^{235}}t_1) - 1$ and $\exp(\lambda_{\mathrm{Th}^{232}}t_1) - 1$, respectively.

Let us assume that neither the Pb isotopes nor U and Th are fractionated (i.e., $l^\alpha{}_{\mathrm{Pb}^{207}} = l^\alpha{}_{\mathrm{Pb}^{208}}$ and $L^\alpha{}_{\mathrm{Th}^{232}} = L^\alpha{}_{\mathrm{U}^{235}}$). We can then drop the subscripts on l and L. The justification of $L^\alpha{}_{\mathrm{U}^{235}} = L^\alpha{}_{\mathrm{Th}^{232}}$ is somewhat difficult. If phase β is closed ($R^\beta = 1$), and if pure daughter loss takes place for samples with fixed $y^\alpha{}_B/x^\alpha{}_B$, the trajectory of $(r_{\lambda_{\mathrm{U}^{235}}}, r_{\lambda_{\mathrm{Th}^{232}}})$ is a straight line of slope

$$\frac{dr_{\lambda_{\mathrm{Th}^{232}}}}{dr_{\lambda_{\mathrm{U}^{235}}}} = \frac{y_B{}^\alpha[\exp(\lambda_{\mathrm{Th}^{232}}t) - \exp(\lambda_{\mathrm{Th}^{232}}t_1)]}{x_B{}^\alpha[\exp(\lambda_{\mathrm{U}^{235}}t) - \exp(\lambda_{\mathrm{U}^{235}}t_1)]} \qquad (8)$$

and passing through the point $[\exp(\lambda_{\mathrm{U}^{235}}t) - 1, \exp(\lambda_{\mathrm{Th}^{232}}t) - 1]$.

Similarly, for pure parent loss from phase α, the trajectory as calculated from (7) has a slope for small losses equal to that given above. A combination of parent and daughter loss for small losses will then lie in a narrow linear region. For large parent losses there is a distinct departure from linearity because the term L^α occurs in the denominator.

Various trajectories calculated from (7) are shown in Figure 8. If the system consists of a high Th/U mineral which is easily disturbed, such as thorite, and a zircon which is not as easily disturbed, the trajectories to be expected would be like line B. The numbers associated with the points on the lines correspond to the value of $l^\alpha x_B{}^\alpha$. This is the maximum displacement ($l^\alpha = 1$) from the intersection with concordia for a two-phase system with a mole fraction x^α of the U in phase α. For example, a system with $x^\alpha = 0.25$ and $y^\alpha/x^\alpha = 2$ can move down curve B only as far as $l^\alpha x^\alpha = 1/4$, corresponding to complete daughter loss from this phase.

Curve C goes to the end point (6.29, ∞), because as a limit one-half of the U must occur in phase β. An example of the trajectories for combined parent and daughter loss using (7) are shown by curves B and E. For a system with

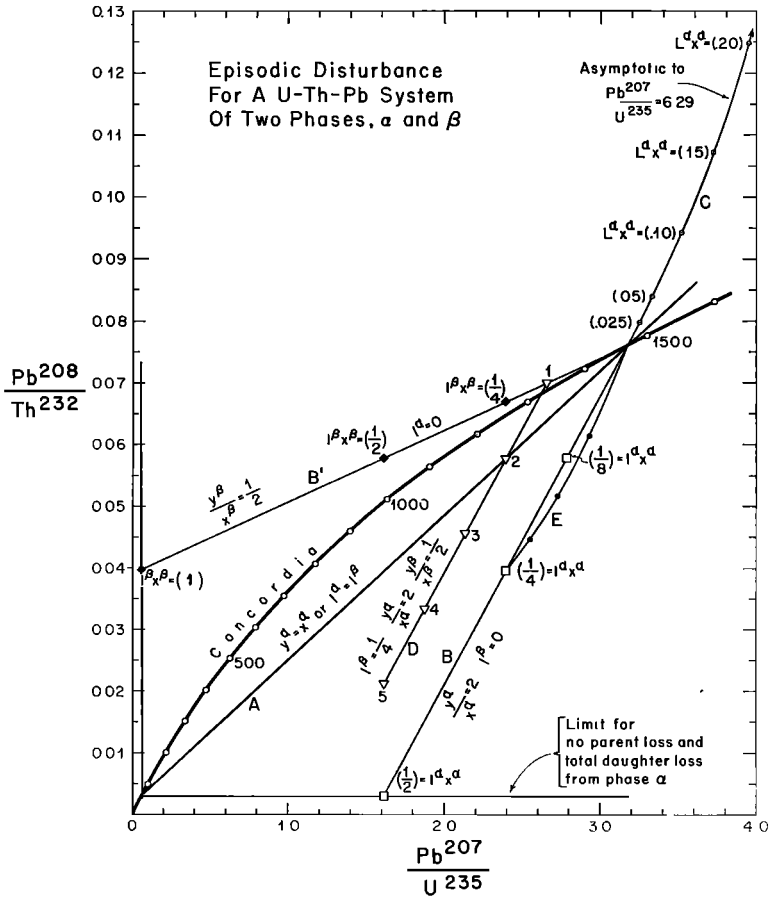

Fig. 8. An ($r_{\lambda_{U^{238}}}$, $r_{\lambda_{Th^{232}}}$) diagram showing various discordia trajectories for a two-phase system subjected to episodic loss with no fractionation from each phase. Line A is for the same fractional loss of daughter from both phases, or for $x^\alpha = y^\alpha$. Lines B and B′ are for daughter loss from only one of the two phases: line B represents loss from phase α with $y_B{}^\alpha/x_B{}^\alpha = 2$, and line B′ represents loss from phase β with $y_B{}^\beta/x_B{}^\beta = \frac{1}{2}$. Line C is for pure parent loss from phase α with $y_B{}^\alpha/x_B{}^\alpha = 2$. Line D is for daughter loss from both phases, the loss from β being 25% and $x^\beta = 2/3$, $y^\beta = 1/3$. The points 1, 2, 3, 4, and 5 correspond to $l^\alpha = 0$, 1/4, 1/2, 3/4, and 1. Note the intersection with the concordia curve. Line E is for parent loss from a phase α which already had daughter loss. The solid points correspond (from bottom to top) to 25, 50, and 75% parent loss. Note that y^α/x^α is the enrichment factor, i.e., the Th/U ratio in phase α compared with the Th/U ratio of the total system.

$y_B{}^\alpha/x_B{}^\alpha = 2$ and $x_B{}^\alpha = 1/4$, complete daughter loss will give the $l^\alpha x^\alpha = 1/4$ point on line B. If, however, parent loss also takes place, the trajectory of total daughter loss and varying degree of parent loss is given by curve E. Line D is for a 25% loss of daughter from phase $\beta(l^\beta = 1/4)$ and various daughter losses from phase α for $x^\alpha = 1/3$. The lowest point is for complete daughter loss.

From a linear array of experimental points consisting of two phases, it follows, if the losses are from one phase (α), that the slope determines $y_B{}^\alpha/x_B{}^\alpha$, and hence, if the ratios $(Th^{232}/U^{238})_\alpha$ and $(Th^{232}/U^{238})_\beta$ are known, the relative proportions of Th and U contributed by each of the phases can be calculated from the equation

$$y^\alpha = \frac{(Th_\alpha{}^{232}/U_\alpha{}^{238})/(Th_\beta{}^{232}/U_\beta{}^{238}) - \dfrac{y^\alpha}{x^\alpha}}{(Th_\alpha{}^{232}/U_\alpha{}^{238})/(Th_\beta{}^{232}/U_\beta{}^{238}) - 1}$$

If, during episodic loss from both phases, phase α is almost completely depleted in both

daughter and parent, or if there is only a very small contribution of U and Th to the system from phase α, and again assuming that neither the Pb isotopes nor U and Th are fractionated, then from (7)

$$r_{\lambda_{Th^{232}}}(t) \approx \frac{(1-l^\beta)}{(1-L^\beta)} \cdot\left\{1+\left[\frac{(1-l^\alpha)}{(1-l^\beta)}-\frac{(1-L^\alpha)}{(1-L^\beta)}\right]\frac{y_B{}^\alpha}{y_B{}^\beta}\right\} \cdot\{\exp(\lambda_{Th^{232}}t)-\exp(\lambda_{Th^{232}}t_1)\} + \exp(\lambda_{Th^{232}}t_1)-1 \quad (9)$$

$$r_{\lambda_{U^{238}}}(t) \approx \frac{(1-l^\beta)}{(1-L^\beta)} \cdot\left\{1+\left[\frac{(1-l^\alpha)}{(1-l^\beta)}-\frac{(1-L^\alpha)}{(1-L^\beta)}\right]\frac{x_B{}^\alpha}{x_B{}^\beta}\right\} \cdot\{\exp(\lambda_{U^{238}}t)-\exp(\lambda_{U^{238}}t_1)\} + \exp(\lambda_{U^{238}}t_1)-1$$

where

$$\frac{(1-L^\alpha)}{(1-L^\beta)}\frac{x_B{}^\alpha}{x_B{}^\beta} \ll 1 \qquad \frac{(1-L^\alpha)}{(1-L^\beta)}\frac{y_B{}^\alpha}{y_B{}^\beta} \ll 1$$

From (9) it follows that the displacements from the episodic line are

$$\delta r_{\lambda_{Th^{232}}} \approx \frac{(1-l^\beta)}{(1-L^\beta)} \cdot\left[\frac{(1-l^\alpha)}{(1-l^\beta)}-\frac{(1-L^\alpha)}{(1-L^\beta)}\right]\frac{y_B{}^\alpha}{y_B{}^\beta} \cdot\{\exp(\lambda_{Th^{232}}t)-\exp(\lambda_{Th^{232}}t_1)\} \quad (10)$$

$$\delta r_{\lambda_{U^{238}}} \approx \frac{(1-l^\beta)}{(1-L^\beta)} \cdot\left[\frac{(1-l^\alpha)}{(1-l^\beta)}-\frac{(1-L^\alpha)}{(1-L^\beta)}\right]\frac{x_B{}^\alpha}{x_B{}^\beta} \cdot\{\exp(\lambda_{U^{238}}t)-\exp(\lambda_{U^{238}}t_1)\}$$

The displacements go to zero for $l^\beta = 1$. The slope of the displacement for the case treated in (9) is given everywhere by

$$\frac{\delta r_{\lambda_{Th^{232}}}}{\delta r_{\lambda_{U^{238}}}} = \frac{\{\exp(\lambda_{Th^{232}}t)-\exp(\lambda_{Th^{232}}t_1)\}}{\{\exp(\lambda_{U^{238}}t)-\exp(\lambda_{U^{238}}t_1)\}}\frac{(Th/U)^\alpha}{(Th/U)^\beta} \quad (11)$$

Since the amount and discordance of phase α remaining in a sample would be variable, it is clear that for this case an exact straight line could not be expected in natural assemblages, but only a band above or below the line t_1t.

For a two-phase system with no parent loss (possibly zircons), we obtain from (7)

$$r_{\lambda_{Th^{232}}} - \exp(\lambda_{Th^{232}}t) + 1 = -[\exp(\lambda_{Th^{232}}t)-\exp(\lambda_{Th^{232}}t_1)] \cdot(y_B{}^\alpha l^\alpha + y_B{}^\beta l^\beta)$$
$$r_{\lambda_{U^{238}}} - \exp(\lambda_{U^{238}}t) + 1 = -[\exp(\lambda_{U^{238}}t)-\exp(\lambda_{U^{238}}t_1)] \cdot(x_B{}^\alpha l^\alpha + y_B{}^\beta l^\beta) \quad (12)$$

If l^α and l^β go to zero simultaneously, the trajectory will pass through [exp $(\lambda_{U^{238}}t) - 1$, exp $(\lambda_{Th^{232}}t) - 1$]. The slope of the line segment connecting this point and an arbitrary point $(r_{\lambda_{U^{238}}}, r_{\lambda_{Th^{232}}})$ is

$$\frac{[r_{\lambda_{Th^{232}}} - \exp(\lambda_{Th^{232}}t)+1]}{[r_{\lambda_{U^{238}}} - \exp(\lambda_{U^{238}}t)+1]} = \frac{[\exp(\lambda_{Th^{232}}t)-\exp(\lambda_{Th^{232}}t_1)]}{[\exp(\lambda_{U^{238}}t)-\exp(\lambda_{U^{238}}t_1)]} \cdot\frac{(y_B{}^\alpha l^\alpha + y_B{}^\beta l^\beta)}{(x_B{}^\alpha l^\alpha + x_B{}^\beta l^\beta)} = \left(\frac{U_\Sigma^{235}}{Th_\Sigma^{232}}\right)_{today}\frac{\Delta\ Pb^{208}}{\Delta\ Pb^{207}}$$

where Σ stands for the total system and $\Delta Pb^{208}/\Delta Pb^{207}$ is the ratio of the number of Pb^{208} and Pb^{207} atoms lost at t_1. If $(Th/U)_\alpha/(Th/U)_\beta > 1$ and $l^\alpha > l^\beta$, the factor $(y_B{}^\alpha l^\alpha + y_B{}^\beta l^\beta)/(x_B{}^\alpha l^\alpha + x_B{}^\beta l^\beta)$ is greater than unity. An assembly of samples, each consisting of mixtures with somewhat varying Th/U ratios, will define a narrow wedge converging on the primary age if the degree of discordance increases with the Th/U ratio of the sample.

In all the discussion of a two-phase system we have emphasized the episodic mode because of its simplicity. The same intrinsic behavior is, of course, manifested by polycomponent systems governed by continuous diffusion loss.

The interpretation of the degree of discordance for the U-Pb system as a function of the concentration of radioactivity in the samples is considerably altered for a multiphase system. For simplicity, we will continue to discuss a two-phase system for an episodic diffusion model. The extension to continuous diffusion is obvious.

Let us define a set of parameters which include the concentrations of U and Th, since these are critical to any discussion of discordance. Define m_α, m_β as the mass fractions of phase α and β which constitute the total system, and c_α, c_β as the concentration of U in each phase. Then

$$m_\alpha + m_\beta = 1 \tag{13}$$

$$x^\alpha = \frac{m_\alpha c_\alpha}{m_\alpha c_\alpha + m_\beta c_\beta} \qquad x^\beta = \frac{m_\beta c_\beta}{m_\alpha c_\alpha + m_\beta c_\beta}$$

(It is clear that x^α is close to 1 for large values of c_α/c_β unless m_α is very small.)

The average concentration $\bar{c}$ is then

$$\bar{c} = m_\alpha c_\alpha + m_\beta c_\beta = c_\beta + m_\alpha(c_\alpha - c_\beta) \tag{14}$$

It follows from (13) and (14) that $\bar{c}x^\alpha = m_\alpha c_\alpha$, $\bar{c}x^\beta = m_\beta c_\beta$, and $m_\beta c_\beta / x^\beta = m_\alpha c_\alpha / x^\alpha$. From the determination of $\bar{c}$ and x^α, we can calculate $m_\beta c_\beta = x^\beta \bar{c}$ and $m_\alpha c_\alpha = x^\alpha \bar{c}$. If two suites of mixtures of these two phases have known average concentrations $\bar{c}$ and $\bar{c}'$, then $m'_\beta/m_\beta = x'^\beta \bar{c}'/x^\beta \bar{c}$, and $m'_\alpha/m_\alpha = x'^\alpha \bar{c}'/x^\alpha \bar{c} = (1 - m'_\beta)/(1 - m_\beta)$. These two equations permit the calculation of m_β, m'_β and hence of c_β, c_α.

For this two-phase system, the function R is the average for the whole sample and will be indicated by a bar. Neglecting parent loss, we have

$$\bar{R} = \frac{r_\lambda - e^{\lambda t_1} + 1}{e^{\lambda t} - e^{\lambda t_1}}$$

$$= x_B{}^\alpha h(u^\alpha/a_\alpha{}^2) + x_B{}^\beta h(u^\beta/a_\beta{}^2) \tag{15}$$

where $h(x) = 6g(x)/\pi^2$.

The critical parameters are the degree of discordance h of each phase and the mole fraction of the total U in each phase. As shown above, these parameters are, respectively, functions of the concentrations of radioactivity and of the concentrations of U and the masses of the phases. $h(u/a^2)$ is a monotonically decreasing function of its argument and is strongly nonlinear. Mixtures of phases with different diffusion parameters will have $\bar{R}$ values intermediate between those of the end members. However, $\tilde{u}/a^2$, defined to be the root of the equation $\bar{R} = h(\tilde{u}/a^2)$ used in the simple one-phase model, will have a dependence on the other parameters x^α, c_α, and c_β unless $u^\alpha/a_\alpha{}^2$ is close to $u^\beta/a_\beta{}^2$. The dependence on the other parameters completely alters the functional dependence of the degree of discordance with the average U and Th concentrations, as was shown observationally to be the case in the section on Pb-U results.

For simplicity in the discussion, we take $a_\alpha{}^2 = a_\beta{}^2$ and let $u^\alpha = qc_\alpha(1 + \gamma)$. q is the proportionality constant between the concentration of radioactivity and the diffusion parameter. $c_\alpha(1 + \gamma)$ is defined to be the total α activity, including the contribution of Th.

If we write $\bar{R}$ in terms of concentrations, we obtain

$$\bar{R} = \frac{m_\alpha c_\alpha h(u^\alpha/a^2) + m_\beta c_\beta h(u^\beta/a^2)}{m_\alpha c_\alpha + m_\beta c_\beta}$$

$$= \frac{c_\alpha h(u^\alpha/a^2) - c_\beta h(u^\beta/a^2)}{c_\alpha - c_\beta}$$

$$+ \frac{c_\alpha c_\beta [h(u^\beta/a^2) - h(u^\alpha/a^2)]}{\bar{c}[c_\alpha - c_\beta]} \tag{16}$$

and

$$\frac{d\bar{R}}{d\bar{c}} = \frac{-c_\alpha c_\beta [h(u^\beta/a^2) - h(u^\alpha/a^2)]}{\bar{c}^2[c_\alpha - c_\beta]}$$

Let us now investigate the consequences of erroneously assuming that the change in $\bar{R}$ is due to a continuous change in concentration in a one-phase system when in fact the systems consist of two phases mixed in various proportions. This implies that $\bar{R}(x^\alpha) = h(\tilde{u}/a^2)$ and demands that $\delta\bar{R}(x^\alpha) = \delta h(\tilde{u}/a^2)$. It follows from (16) and the definition of h that

$$\frac{d \ln (\tilde{u}/a^2)}{d \ln \bar{c}} = \frac{\bar{c} d(\tilde{u}/a^2)}{(\tilde{u}/a^2)\, d\bar{c}}$$

$$= \frac{c_\alpha c_\beta [h^\beta - h^\alpha]}{6\bar{c}[c_\alpha - c_\beta] \dfrac{\tilde{u}}{a^2} \displaystyle\sum_{m=1}^{\infty} e^{-m^2\pi^2\tilde{u}/a^2}} \tag{17}$$

This expression is the fractional increase in $\tilde{u}/a^2$ calculated in order to account for a fractional change in $\bar{c}$ due to mixing. The denominator vanishes for $\tilde{u}/a^2 = 0$ and in the limit as $\tilde{u}/a^2 \to \infty$. When the logarithmic derivative (equation

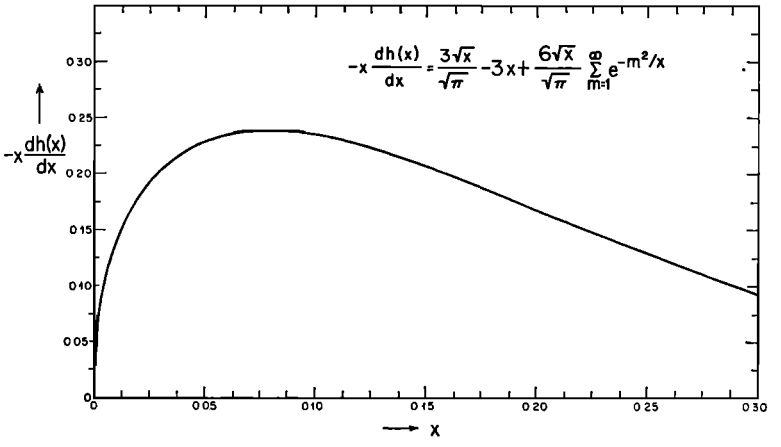

Fig. 9. Graph of the function $-xdh(x)/dx$, where

$$h(x) = \frac{6}{\pi^2} g(x) = \frac{6}{\pi^2} \sum_{m=1}^{\infty} \frac{e^{-m^2\pi^2 x}}{m^2}$$

17) is greater than unity, it follows that the calculated fractional change in $\bar{u}/a^2$ is greater than the fractional change in observed concentration. See Appendix B for an approximate expression of the function

$$-(\bar{u}/a^2)6 \sum_{m=1}^{\infty} e^{-m^2\pi^2\bar{u}/a^2} = x\frac{dh(x)}{dx}.$$

A graph of this function is given in Figure 9.

Discussion of Experimental Results

In terms of a one-phase system, the data presented in Figure 3 indicate preferential Th^{232} daughter loss, although the physical and chemical processes which could cause this are not at all clear. It does not seem reasonable to attribute the observed effects to preferential loss of intermediate daughter products in the Th decay series because of the short half-lives of these nuclides. Evidence has been presented for loss of intermediate daughter products for the U^{238} series from zircons [*Doe and Newell*, 1965] and for the Th^{232} series from thorite [*Senftle et al.*, 1956]. However, there is no significant difference in the energies of the α particles in the Th decay series which would cause a greater recoil to the Pb^{208} nucleus and its progenitors as compared with the two U series. If, following the earlier discussion of a one-phase system, we interpret the effect shown in Figure 3 as due to the preferential diffusion of Pb^{208} over Pb^{206} and Pb^{207}, we calculate $D_{Pb^{208}}/D_{Pb^{207}} = 1.19$ for this suite of zircons. Simple isotopic fractionation should be far less than this, and it therefore appears that some other process must be responsible for this apparent observed enhancement in $D_{Pb^{208}}$. The addition of Th to a one-phase system could have this effect, but this would demand that the amount of Th added is related to the U and Th contents in a regular way. It is possible that the number of lattice sites that could accept additional U and Th is related to the number of defects that are approximately proportional to the original U and Th contents because of the induced radiation damage. *Gruenenfelder* [1963], for example, has demonstrated the presence of large amounts of water in the U-rich, strongly discordant fraction of a cogenetic zircon concentrate. If this is hydration due to radiation damage, as is well known for the more extreme case of thorite, the disturbed structure must have fundamentally different chemical properties from the undamaged material.

If the zircon separates used in this study represent a multiphase assemblage because of the presence of impurities and of phases of zircons of different Th/U ratios, we then have to interpret the experimental results presented in Figures 3 and 4 in the light of our discussion of the two-phase model in the preceding section.

It is obvious from this discussion that any preferential loss from one particular phase of a multiphase system, due to diffusion in nature or

to loss during handling in the laboratory, would have a profound effect on the array of data in a Th-U-Pb diagram.

The presence of minerals such as thorite, which have extremely high concentrations of radioactive elements, may tend to dominate the behavior of the mineral separates analyzed. If such minerals lose daughter products readily, their ($r_{\lambda U^{238}}$, $r_{\lambda U^{235}}$) systematics may be disturbed to some extent, causing the data points to move toward the origin, but this effect may dominate the observed deviations in the Th-U-Pb system. The relative concentrations of the radioactive elements Th and U in minerals such as thorite may be between 10^4 and 10^3 times as great as they are in zircons. This means that if a zircon concentrate contains one grain in a thousand of thorite which has a Th/U ratio of 6, and if the zircon has 300 ppm U and 150 ppm Th, only 18% of the total Th and 72% of the total U are in the zircon. Great care must therefore be taken in correlating degree of discordance with U and Th content in Pb-U systems containing radioactive impurities.

The effects of contributions of Th and U by minor quantities of uranothorite were first recognized by *Silver and Deutsch* [1961, 1963], who subsequently subjected all zircon concentrates to a 1-hour acid-washing treatment with hot (80°C) concentrated HNO_3, which dissolves the uranothorite. All samples reported in this paper were subjected to the following washing treatment with hot (80°C) acid: 20 min in 35% HNO_3, 20 min in 3.1 *N* HCl, and, finally, 20 min in Pb-free 35% HNO_3 before analysis. This treatment removes pyrite, apatite, and surficial iron oxide stains. Although this treatment appears to destroy thorite grains, inclusions of thorite, apatite, or other minerals which are in the interiors of the individual zircon crystals would at best be only partially attacked. Unless the treatment completely removes some of these phases or does not disturb them at all, the distinction between certain geologic processes and the laboratory handling will be impossible.

Tilton [1956] showed that the loss of Pb isotopes occurring during acid washing of a given sample was not necessarily in proportion to their abundance in the total sample. He observed a Pb^{208}/Pb^{206} ratio of the radiogenic Pb in the acid wash of the Tory Hill zircon which was seven times larger than the same ratio in the unwashed sample. *Silver and Deutsch* [1963] pointed out that thorite may have been present in this particular zircon separate, as indicated by the unusually high Th/U ratio for the unwashed sample. In a thorough investigation, these authors studied the effects of acid-wash treatments on zircons. The presence of a highly radioactive mineral in the unwashed zircon separates was established by autoradiography and identified as uranothorite. From analysis of the acid-wash solution, these authors inferred that highly discordant uranothorite was dissolved. The U and Pb concentrations and the Pb isotopic ratios of an aliquot of handpicked zircons were compared with an aliquot from the same size fraction washed in hot HNO_3. The concentration of U and radiogenic Pb was 2 to 3% higher in the handpicked fraction, whereas the ratio of radiogenic Pb^{208}/Pb^{206} was 15% higher. Silver and Deutsch inferred from this that there was possibly a very small uranothorite residue in the hand-picked sample. On the other hand, since the specific α activities showed no difference between hand-picked and acid-washed samples of similar fractions [*Silver and Deutsch*, 1963, Figure 4], it was concluded that both methods are essentially equally effective for the removal of thorite. It appears to us that these results may just as well indicate a possible preferential leaching effect of Pb during the acid-wash treatment from metamict zircons of high Th/U ratio. A similar argument could be made from their experiments with two zircon aliquots which were subjected to acid washings of increasing intensity. The ratio of radiogenic Pb^{208}/Pb^{206} in the mildly treated aliquot is 10% higher. It was also shown that acid treatment lasting for 1 and 14 hours, respectively, gave essentially the same Pb^{208}/Pb^{206} ratio for the residue. It is not clear from these data whether all the thorite has been dissolved or if only the Pb has been removed. This washing procedure appears to be reasonably safe for the Pb-U system according to Silver and Deutsch. However, it is not known at the present time whether the commonly used acid-wash procedures are also satisfactory for the combined U-Th-Pb system. The microprobe results presented in this paper indicate that this method dissolves at least 90% of the thorite grains present, but it is not clear what undesirable side effects the acid washing may have, in particular with respect to preferential leaching

of daughter from highly metamict zircon or thorite phases with high Th/U ratios. From the techniques used for the etching of fission tracks [*Fleischer et al.*, 1965], it is suggestive that the reagents used should not attack unmetamict zircon. Any preferential leaching effects will immediately show up by departures in the Th-U-Pb system (see Figure 8). They may remain unnoticed in the U-Pb system, where they will essentially change the degree of discordance.

For a real understanding of the Th-U-Pb systems it is imperative that the distribution of the radioactive elements in the zircon concentrates and the crystals themselves be known. For this reason 200 grains from each of four acid-washed separates, for which Th ages had been measured, were scanned by electron microprobe to determine whether there were any grains or inclusions of high U or Th contents. The samples were scanned with a broad electron beam ($\approx$10 μ diameter). All grains or inclusions whose zirconium contents were significantly less than that of a typical zircon were particularly examined, and it was found that the U and Th contents of such grains were very low. In addition, all observed impurities (totaling about 10 grains each) in 30-mg fractions (containing about 3×10^4 individual zircon grains) of the acid-washed separates $\beta 1$ and $\beta 2$ were removed by hand and examined on the probe. These grains were all low in Zr, U, and Th, as compared with zircons. The presence of thorite in the original unwashed sample was verified by analysis of impurities hand picked from a +120-mesh

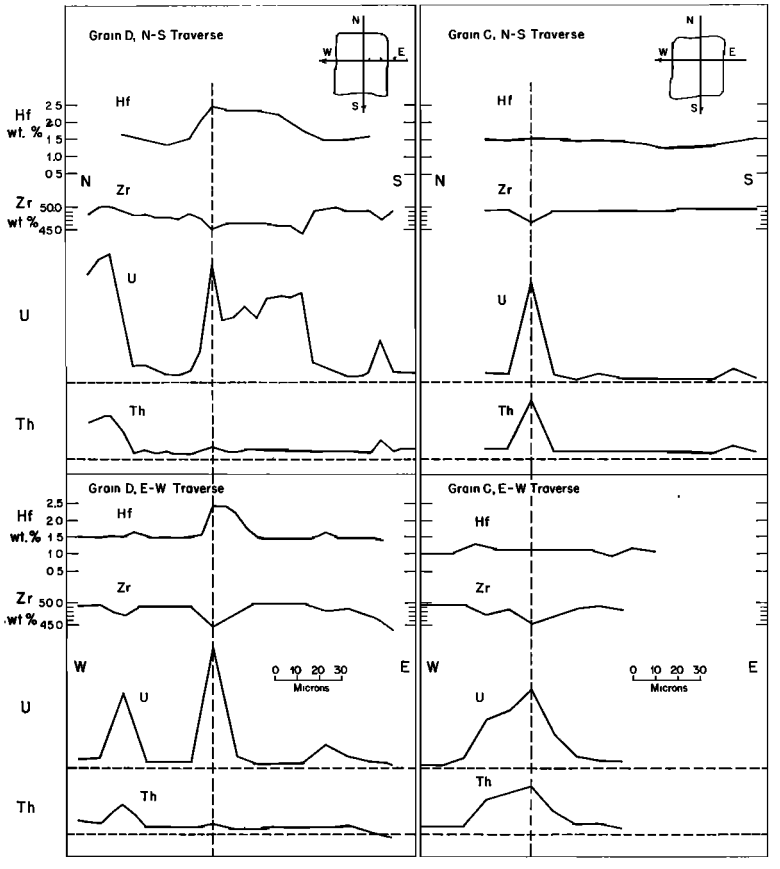

Fig. 10. Electron microprobe analyses for U, Th, Zr, and Hf across sections perpendicular to the *c* axes of two zircon grains (not acid-washed). The dashed vertical line indicates the intersection between two perpendicular traverses. The inset sketches illustrate the directions of the traverses (i.e., N-S or E-W). Approximate base lines are indicated for the elements U and Th.

zircon concentrate. Ten thorite grains which have Th contents of over 70 wt % and Th/U ratios ranging from 5 to 12 were found in approximately 100 mg of the zircon concentrate. This constitutes a very significant fraction of the Th and U in the unwashed sample.

A more detailed study of U, Th, and Zr was made on three zircon grains from each of the acid-washed separates $\beta 1$ and $\beta 2$. Some grains of the +120-mesh fraction which had not been subject to any acid washing were analyzed for U, Th, Zr, and Hf. Traverses both perpendicular and parallel to the c axes of the crystals were taken using a beam of 2 μ. In some grains considerable variations of both the U and Th concentration (up to a factor of 10) were found, the Th/U ratio ranging up to a factor of 4 (Figure 10). The limited observations made in this study appear to indicate higher concentrations in hot spots rather than in concentric growth zones. Other grains show a relatively uniform distribution of the radioactive elements, and the low concentrations observed compare with those found outside the hot spots of the inhomogeneous zircon crystals. No gross differences in U and Th were observed between the acid-washed and unwashed separates, except for one unwashed grain (Figure 10, grain D) where a marked increase in U and Th was observed on one exterior surface. In general, the U and Th variations were sympathetic and the Zr decreased with increasing U and Th. This anticorrelation with Zr was also found for Hf (Figure 10). This observation suggests that U and Th substitution may be correlative with Hf substitution in the zircon lattice.

The local areas in which U and Th were more concentrated did not show any dominance of Th over U. It is possible that these hot spots represent a different phase of zircon. On the other hand, they may be due to small inclusions of other minerals that are incompletely resolved by the microprobe. Of the inclusions which were optically recognized, none showed high U or Th contents. Many of these inclusions appear to be apatite, as judged by their habit. From the preceding microprobe observations, we conclude (1) that the unwashed mineral concentrates contain about 1 grain of thorite per 10^3 grains of zircon; (2) that the acid-washed fractions of the analyzed samples $\beta 1$ and $\beta 2$ were free of loose thorite grains (i.e., the ratio of the zircon grains to individual thorite grains is greater than about 3×10^4); (3) that among the 800 zircons examined no grains were found which had obvious (i.e., more than 10% of volume of the zircon crystal) inclusions of thorite, which defines an upper limit of about 1 part of thorite in 10^4 parts of zircon; and (4) that the zircon crystals themselves are rather low in radioactivity except for frequent inclusions of what appears to be a minor zircon phase distinct by its relatively high Hf content. These inclusions seem to contribute a significant portion to the total U and Th content of the zircons, and they also show considerable variation in their Th/U ratios.

The experimental data for the Sandia zircons (see Figure 3) may be explained in several ways. In the light of the microprobe investigation and the analytical results listed in Table 1, we conclude that the deviations of the data points from the theoretical diffusion trajectories must be due to the fact that the samples analyzed are multiphase assemblages.

In Figure 6 several trajectories are explored for simple two-phase systems. From this it appears that the Sandia data may be explained by assuming that the analyzed fractions are zircon concentrates containing either small amounts of a highly discordant phase that has high Th/U ratios or a larger portion of a relatively discordant phase that has a slightly high Th/U ratio. However, it is not well understood why such mixtures should happen to plot on a straight line intersecting concordia at the point of primary age unless the concentrations, composition, and discordance of the accessory phases were favorably correlated with the discordance of the zircons.

The presence of one grain of highly discordant thorite per 3×10^4 grains of zircon in sample $\beta 2$ would fully explain the departure of this data point from an episodic or continuous diffusion trajectory. On the other hand, if the same contamination were assumed for the other sample concentrates, the data points would plot on a straight line which originates from a point on the diffusion trajectory corresponding to the thorite and which intersects concordia at a point above the primary age, as determined from the U-Pb diagram (Figure 1). This case is illustrated by line B of Figure 11. This line is for zircon concentrates b_n of variable discordance to which a constant proportion of 90% discordant thorite

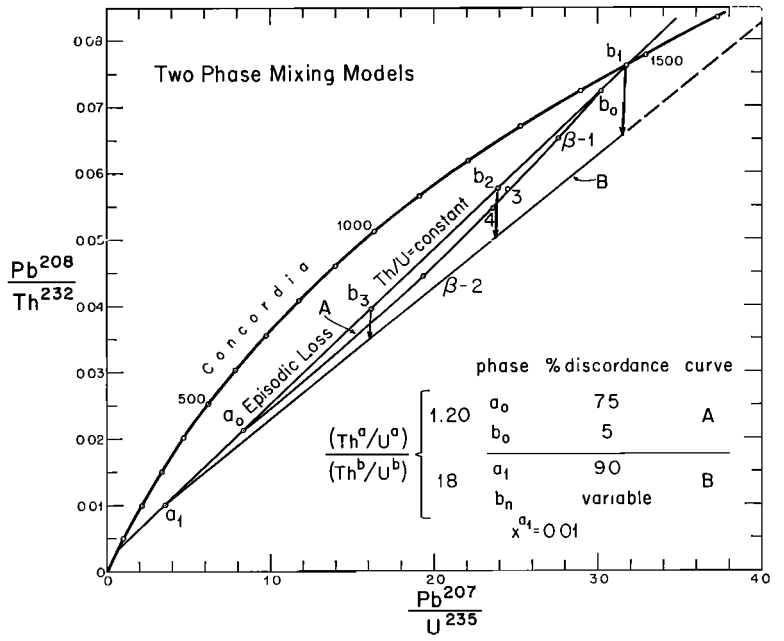

Fig. 11. An ($r_{\lambda_{U^{235}}}$, $r_{\lambda_{Th^{232}}}$) diagram showing mixing models for two phases a and b with different $(Th^a/U^a)/(Th^b/U^b)$ ratios. Curve A is a mixing curve between a 5% discordant zircon phase b_0 and a 75% discordant ($l^a = 0.75$) zircon phase a_0. Note the close fit of this simple two-phase model with the observed data points of the Sandia zircons. The arrows indicate the direction in which the Th-U-Pb systems will be displaced if 90% discordant ($l^a = 0.9$) thorite a_1 is added to zircon phases b_n of variable discordance. Line B connects the points attained by the addition of a *constant* proportion [$x^a = U^a/(U^a + U^b)$] of this thorite to the zircon phases indicated. This line intersects concordia at time $t^+ > t$.

a_1 is added. The assumed value for x^{a_1} (i.e., the mole fraction of the total U in the concentrate which is contributed by the thorite) is highly exaggerated for clarity. To explain the observed data by the presence of highly discordant thorite, it would be necessary to assume that the amount of thorite present or its degree of discordance was proportional to the degree of discordance of the zircons. This would appear to be a somewhat contrived explanation. The data point by *Tilton* [1962], which plots on the convex side of concordia (see Figure 3), has to be interpreted either in terms of Figure 6 or Figure 8. This sample may represent a mixture between a relatively discordant zircon phase that has a low Th/U ratio and a more concordant phase that has a high Th/U ratio (curve B in Figure 6). A sample concentrate consisting of a mixture of two phases, of which the phase with the low Th/U ratio has lost daughter product preferentially, would also plot on the convex side of concordia (compare point 1, line D in Figure 8).

It was also observed that a linear correlation exists between the Th/U ratio of the Sandia samples and the vertical displacement of the data points from the episodic diffusion trajectory. From this the Th/U ratio for a concordant zircon can be obtained by extrapolation. It corresponds to about 0.41.

Examination of the data for different fractions presented in Table 1 shows that in most cases the degree of discordance and the Th/U ratio increase with the U concentration. The total spread in the Th/U ratio for the six samples is about 20%. If this increase in Th were due to the addition of discordant (60-m.y.) thorite alone, it would clearly overcompensate the observed offset from the episodic line. We therefore conclude that the Th/U ratio of the zircon grains themselves increases with the degree of discordance.

From the microprobe data it would appear that a large part of the radioactivity in the Sandia zircons is concentrated in hot spots and

the rest of the crystal is relatively low in U and Th. Preliminary microprobe data on the distribution of Pb indicate that high concentrations of this element do not necessarily follow those of the U and Th. This in turn is suggestive that many of the hot spots are highly discordant. This observation raises the interesting possibility that the zircon concentrates, and indeed single zircon crystals, may be regarded as mixtures of an essentially concordant low U and Th zircon phase and a discordant high U and Th zircon phase (hot spots), with a slightly higher (about 20%) Th/U ratio on the average. Such a situation is illustrated by curve A in Figure 11. The upper part of this curve deviates only slightly from the best-fit straight line through the observed data points.

Gruenenfelder [1963] obtained zircon separates with widely different U concentrations and degrees of discordance by a hand-picking procedure. He demonstrated that the conventional methods of separation (using sieves and a Frantz separator) yielded zircon separates which were intermediate mixtures of rather limited variation of the more extreme separates obtained by hand picking. It is certain that the most extreme fractions which Gruenenfelder obtained were themselves inhomogeneous in their U concentration. Nonetheless we infer from our own observations on the Sandia samples and those reported by Gruenenfelder that some concentrates of cogenetic zircon may be regarded as mixtures of extremely radioactive zircons and zircons with low radioactivity. In the extreme case of such a two-component system, the observations that the Pb-U (not the Pb-U-Th system) data lie on a straight line would be the trivial result of a mixing of end members and not be due to a continuous change in the degree of discordance. It will therefore be of great importance to establish the relationship of discordance and average (U + equivalent Th) content in sample fractions which each have a relatively uniform concentration of radioactive elements.

We should note here that, although the two-phase model is a gross oversimplification, it will nonetheless tend to dominate the degree of discordance unless the sample population is distinctly unimodal in U + equivalent Th concentration. This result follows because the highly discordant zircons also contribute a large fraction of the total U in the sample, assuming that radiation damage governs the loss of daughter product (see equation 16).

A plausible assumption made in the radiation damage diffusion model by *Wasserburg* [1963] calls for the proportionality of the diffusion

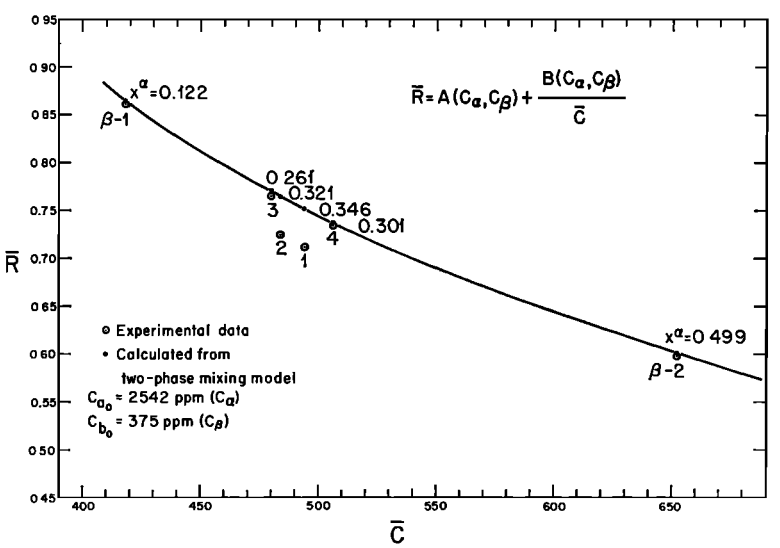

Fig. 12. Graph of the degree of discordance versus mean U concentration for the samples analyzed, using a two-phase model. $A = [c_\alpha h(u^\alpha/a^2) - c_\beta h(u^\alpha/a^2)]/(c_\alpha - c_\beta)$, $B = c_\alpha c_\beta[h(u^\beta/a^2) - h(u^\alpha/a^2)]/(c_\alpha - c_\beta)$.

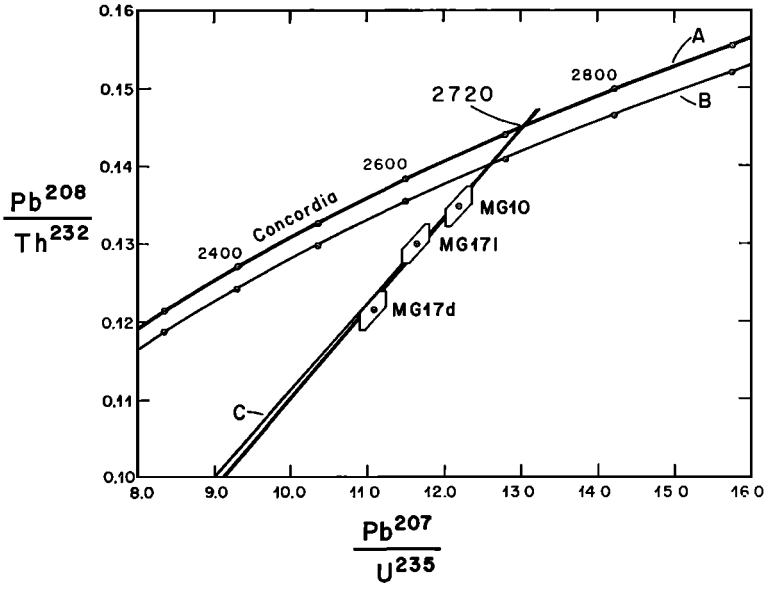

Fig. 13. An ($r_{\lambda_{U^{238}}}$, $r_{\lambda_{Th^{232}}}$) diagram for three zircon samples from a suite of 'Algoman' granites, Manitouwadge, Ontario, Canada [*Tilton and Steiger*, 1965]. Line C connects the origin with the 2720-m.y. point on concordia (see Figure 3).

constant D with the U + equivalent Th concentration. It has been shown in the section on the U-Pb relationships that the experimental data do not satisfy this assumption if the equations for the one-phase system are used. If the samples analyzed are considered as mixtures of a concordant zircon of low radioactivity and a discordant, highly radioactive phase, the correlation between discordance and U concentration can be explained quantitatively. Curve A in Figure 11, which fits the data points, represents a possible mixing curve between a 75% discordant phase a_0 and a 5% discordant phase b_0. Assuming that all analyzed samples are two-phase mixtures of these extreme end members, the value x^{a_0} (i.e., the mole fraction of the total U in the mixture which is contributed by end member a_0) can be determined for each sample. Using (3), (4), (13), and (14) and the respective average U concentrations $\bar{c}$, we obtain the U concentrations c_a and c_b for the two end members of the mixtures by fitting the experimental data to a curve of the form given by (3). From this the average $\bar{R}$ can be calculated for each sample. Figure 12 shows a graph of the calculated $\bar{R}$. For the samples $\beta 1$, $\beta 2$, 3, and 4, a good agreement is obtained between the calculated and the observed values for $\bar{R}$. The experimental points 1 and 2 do not fit this simple model. A much higher concentration of U in phase a would be required or a multiphase system would have to be assumed in order to explain the observed discordance of these two samples. A further comparison shows that the values of U + equivalent Th (Table 3) are identical for the two samples, whereas the Th/U ratio (Table 1) is different by more than 20%. This is in contrast to the observations made for the other samples, where the Th concentrations and the Th/U ratios increase monotonically with the U concentration and the degree of discordance.

It can be shown by equation 3 that the choice of possible end members for the two-phase mixing model is rather limited. We are forced to assume end members which show a large difference in the degree of discordance in order to explain the pseudo-linear array of the data points on an ($r_{\lambda_{U^{238}}}$, $r_{\lambda_{Th^{232}}}$) diagram (Figure 11, curve A). On the other hand, the discordance of phase a_0 cannot exceed 80 to 85% because the values for x^{a_0} will become too small to obtain the required contribution of U from phase a_0. Phase b_0 has to be nearly concordant, with a U concentration c_{b_0} relatively close to the average U concentration of sample $\beta 1$. The U concentration needed in phase b_0 for this model

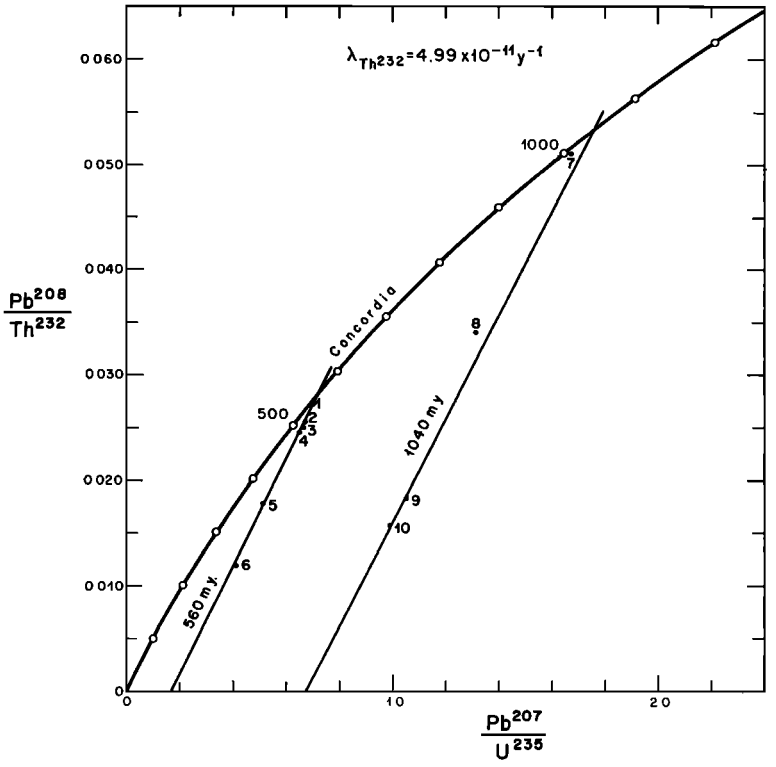

Fig. 14. An ($r_{\lambda_{U^{235}}}$, $r_{\lambda_{Th^{232}}}$) diagram for two suites of zircon samples which have primary ages of 1040 and 560 m.y., respectively, as determined from linear arrays on the ($r_{\lambda_{U^{235}}}$, $r_{\lambda_{U^{238}}}$) diagram. All samples show closely corresponding Pb^{207}/Pb^{206} ages. Data points 1, 2, 3, 6, and 10 are from *Tilton et al.* [1957], 7, 8, and 9 are from *Davis et al.* [1962], and 4 and 5 are from *Wetherill et al.* [1966].

is approximately 350 ppm. This result appears to be considerably greater than the concentration estimated with the microprobe in those regions of the zircon crystal outside the hot spots. This may be due to inaccuracies in instrument calibration or to the assumption of a simple two-phase model.

Of the samples investigated, 1 through 4 represent a size fraction separation, and samples $\beta1$ and $\beta2$, which show the largest difference in discordance, were obtained by magnetic separation from a large zircon concentrate. Samples 3 and 4 lie between $\beta1$ and $\beta2$, as shown in Figure 11. The cause of the increased magnetic susceptibility of sample $\beta2$ is not known. These observations are compatible with the samples being mixtures of more extreme end members, satisfying the assumptions given above. A correlation definitely exists between magnetic susceptibility, discordance, radioactivity, and the Th/U ratios in these particular samples. It was previously shown that the hot spots are correlated with a decrease in Zr. For that reason it will be important to extend the microprobe investigations to other elements, such as Fe, which may have a distinct effect on the susceptibility.

Discussion of Earlier Th-Pb Data

The general effects reported in this paper may be found for a variety of other samples previously reported in the literature. Figure 13 shows the data of *Tilton and Steiger* [1965] and Tilton and Steiger (in preparation) on zircons from Manitouwadge. The intersection on the concordia curve for the ($r_{\lambda_{U^{235}}}$, $r_{\lambda_{Th^{232}}}$) diagram was taken from the intercept on the ($r_{\lambda_{U^{235}}}$, $r_{\lambda_{U^{238}}}$) diagram. These data again appear to form a linear array. Samples MG 17d and MG 17l are different fractions of zircon from the same rock, and sample MG 10 is from another part of the same pluton. A best-fit line is seen to lie somewhat below the line drawn from the origin to the

intersection at concordia. Although there is insufficient spread in the degree of discordance of the data points, they seem to be compatible with those results presented earlier, the time of intersection on concordia corresponding to the primary age as determined from the other diagram.

Figure 14 shows the compilation of data for two different age groups corresponding to primary ages of 1040 and 560 m.y. that were taken from a suite of samples from different localities. Although these are not cogenetic suites, they clearly appear to define a linear array showing an upper intersection on the concordia curve compatible with the U-Pb results. The slopes of these two lines are far greater than those for modern episodic loss, and they may possibly represent a relatively recent loss of Pb from phases having a high y^a/x^a value. This phenomenon may be distinct from that observed for the Sandia granite and the Manitouwadge samples. It appears that these data are best explained by the existence of phases or impurities that have high Th/U ratios in the mineral separates which lost most of their daughter product and only a small amount of parent. Figure 15 illustrates two similar suites of data from the literature for primary ages of 1935 and 2600 m.y., respectively, as determined from the conventional U-Pb diagram. The zircons from the Little Belt Mountains show a large scatter, but the more extreme points lie on a line intersecting the concordia at the time point corresponding to the primary age. The monazite data from South Africa form a linear array which also intersects concordia at the time point of primary age. As in the other cases, the divergence of the two lines from the theoretical diffusion trajectory may be explained by the presence of highly discordant phases with high Th/U ratios (thorite?) in the analyzed mineral concentrates.

Since none of the examples cited in Figures 14

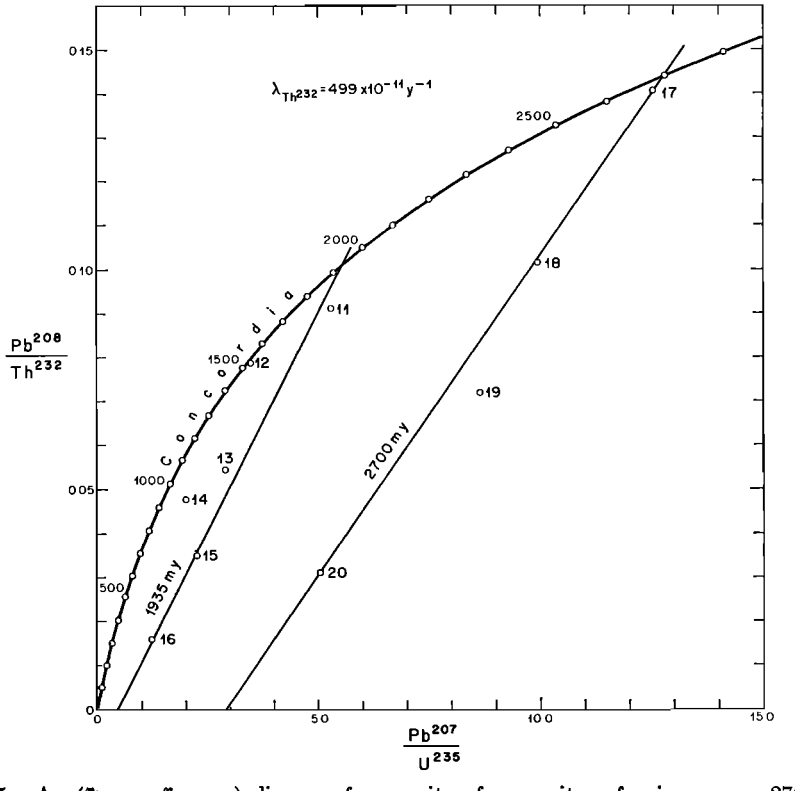

Fig. 15. An ($r_{\lambda_{U^{235}}}$, $r_{\lambda_{Th^{232}}}$) diagram for a suite of monazites of primary age 2700 m.y. [*Holmes*, 1954; *Holmes and Cahen*, 1955] and a suite of zircons of primary age 1935 m.y. [*Catanzaro and Kulp*, 1964]. Primary ages were determined fromli near arrays on the ($r_{\lambda_{U^{235}}}$, $r_{\lambda_{U^{238}}}$) diagram. Generally they are in good agreement with the corresponding Pb^{207}/Pb^{206} ages. The regularities in these monazite data were first observed by *Ahrens* [1955].

and 15 is cogenetic, it is not to be expected that they lie on common mixing curves of the type shown in Figures 6 and 11. It rather appears that each data point belongs to an individual mixing curve of a closely concordant phase and a second phase which has a variable degree of discordance but happens to show a similar enrichment factor y^a/x^a. This case is illustrated by Figure 8, line B.

Other data in the literature [e.g., *Silver and Deutsch*, 1963] indicate a roughly linear array in the ($r_{\lambda U^{***}}$, $r_{\lambda Th^{***}}$) diagram but have an intersection on the concordia curve which appears to have no time significance. The monazite data of *Nicolaysen* [1957] also form a roughly linear array, but it has a very low slope.

It is evident from these observations that the accumulation of more data on cogenetic minerals and mineral suites with well-understood washing procedures and U, Th, Pb distributions will be necessary before a general explanation can be offered.

Conclusions

We have shown that the Th-U-Pb system of a cogenetic suite of zircons from the Sandia Mountain granite exhibits regularities which make it very useful for inferring the history and the composition of these samples. On an ($r_{\lambda U^{***}}$, $r_{\lambda Th^{***}}$) diagram the points appear to lie on a straight line which intersects the concordia curve at the time point corresponding to the primary age of the suite. The line has a slope greater than [exp ($\lambda_{Th^{***}}t$) − 1]/[exp ($\lambda_{U^{***}}t$) − 1] and therefore passes to the right of the origin, i.e., outside the accessible region for a single-phase system subject to nonfractionating daughter loss.

A theoretical analysis of the behavior of single-phase Pb-U-Th systems was made. The experimental data for some natural assemblages of zircon were in disagreement with the single-phase model for both the U-Pb and the Th-U-Pb systems. A theoretical analysis was made of two-phase systems subject to an episodic disturbance. The daughter-parent ratio r_λ for a two-phase system depends on the discordance of each phase and the fraction of the total parent in the sample which is contributed by each phase. Some general relationships were derived for the behavior of the Th-U-Pb systems and for the relationship between discordance and average U + Th concentration. It was shown that the observations are compatible with this model. More generally, it appears that the fundamental behavior of natural systems must be considered in terms of multiphase assemblages in order to explain (1) the functional relationship between the degree of discordance and the average radioactivity and (2) the linear arrays observed for data in the ($r_{\lambda U^{***}}$, $r_{\lambda Th^{***}}$) diagram. The latter diagram clearly shows the effects of multiphase systems because of the fact that the Th/U ratio is not constant in nature. It is evident that a more formal statistical treatment of multiphase assemblages will be necessary before we can discuss natural systems.

Investigation with the electron microprobe demonstrated clearly that the zircon concentrates and the individual zircon crystals from the Sandia granite are indeed multiphase assemblages that have variable U and Th concentrations and Th/U ratios. The radioactive elements appear to be concentrated in local domains of zircon within the zircon crystals themselves. The analytical data indicate that the degree of discordance increases with the increasing average U and Th concentrations [*Silver and Deutsch*, 1963] and with the increasing Th/U ratios. This correlation suggests that the zircon assemblages studied are mixtures of highly discordant (metamict) zircon phases of high radioactivity and relatively concordant zircon phases of low Th and U concentrations and relatively low Th/U ratios.

Linear arrays on the ($r_{\lambda U^{***}}$, $r_{\lambda Th^{***}}$) diagram were also obtained for some other published data. The slopes, however, are usually steeper than those for the Sandia samples, and higher Th/U ratios would be called for in the discordant end member of the mixtures. At the present time it is not known whether the slopes of these apparent straight lines are mainly affected by diffusion over geologic times or by the commonly used acid-washing procedure in the laboratory. Clearly, more experimental work has to be done in this direction. The fact that the Th/U ratio is not constant in natural materials is responsible for the complicated behavior of open Th-U-Pb systems and enables us to obtain important information which the U-Pb system alone cannot provide.

Appendix A

In terms of the episodic diffusion parameter

u/a^2 for pure daughter loss, $dr_{\lambda'}/dr_\lambda = \sqrt{k}\,(e^{\lambda' t} - e^{\lambda' t_1})/e^{\lambda t} - e^{\lambda t_1})$, where $k = u'/u = D'/D$. This result follows for the δ-function approximation. The analytical expression for r_λ for the case of no diffusion loss except in the time interval Δ starting t_1 years ago is given by

$$r_\lambda(t) = (e^{\lambda(t_1-\Delta)} - 1) + (e^{\lambda t} - e^{\lambda t_1})\frac{6}{\pi^2}\sum_1^\infty \exp\left[-n^2\pi^2 D_0\,\Delta/a^2\right]/n^2 + e^{\lambda(t_1-\Delta)}\frac{6}{\pi^2}\sum_1^\infty \frac{[1 - \exp(-n^2\pi^2 D_0\,\Delta/a^2 + \lambda\Delta)]}{n^2(n^2\pi^2 D_0/\lambda a^2 - 1)}$$

$D(t) = D_0$ for the time between t_1 and $t_1 - \Delta$ years ago and is zero otherwise. It follows, therefore, that a calculation of the diffusion parameter u/a^2 in the limit as $\Delta \to 0$ and $D_0\,\Delta \to u$ depends on the behavior of D_0/a^2, which is implied to be infinite in the treatment given by *Wasserburg* [1963]. It remains to be seen whether episodic diffusion losses in the neighborhood of concordia ever satisfy this relationship.

Appendix B

The function

$$dh(x)/dx = -6\sum_1^\infty e^{-m^2\pi^2 x}$$

is closely related to the θ function (θ_3, p. 463 et seq., *Whittaker and Watson* [1920]). It follows that

$$\frac{x\,dh(x)}{dx} = -3\left(\frac{x}{\pi}\right)^{1/2} + 3x - 6\left(\frac{x}{\pi}\right)^{1/2}\sum_{m=1}^\infty e^{-m^2/x}$$

$$\approx -3(x/\pi)^{1/2} + 3x \quad 0 \le x \le 1/10$$

and

$$h(x) \approx 1 - 6(x/\pi)^{1/2} + 3x \quad 0 \le x \le 0.18$$

and

$$h(x) = \frac{6}{\pi^2}\,g(x) = \frac{6}{\pi^2}\sum_{m=1}^\infty \frac{e^{-m^2\pi^2 x}}{m^2}$$

These approximations are more accurate than 0.02% for values of x up to 0.10 and are a convenient means of representing the above functions in simple algebraic form or for calculation. For values of x greater than 0.1, the first few terms in the original series are adequate.

Note added in proof. We wish to thank C. Allègre for calling our attention to the paper by *Ahrens* [1955]. We subsequently found that in his work Ahrens had first used the ($r_{\lambda U^{238}}$, $r_{\lambda Th^{232}}$) diagram. The linear array of the monazite data presented in Figure 15 was in fact first shown by Ahrens. The more general use of coupled parent daughter systems ('la méthode Concordia généralisée') has been presented by *Allègre* [1964] and *Allègre and Michard* [1964] for the (Pa/U, Io/U) and (Sr/Rb, Ar/K) systems.

Acknowledgments. We acknowledge discussions with C. Allègre, G. L. Davis, S. R. Hart, and L. T. Silver. Constructive casual and causal comments by G. R. Tilton were very valuable. We wish to thank Dean Bohnenblust for the use of an old Tauberian device. Most of the analyses reported here were made in the laboratories of the Carnegie Institution of Washington, and we thank L. T. Aldrich for the use of the mass spectrometers. The microprobe analyses were done by A. Chodos, and C. Chase performed many of the computations.

This work was supported by contracts from the Office of Naval Research [Nonr-220(47)], the Atomic Energy Commission [AT(04-3)-427], and grants from the National Science Foundation [GP-5391, GP-2796].

References

Ahrens, L. H., Implications of the Rhodesia age pattern, *Geochim. Cosmochim. Acta, 8,* 1–15, 1955.

Aldrich, L. T., G. L. Davis, and H. L. James, Ages of minerals from metamorphic and igneous rocks near Iron Mountain, Michigan, *J. Petrol., 6,* 445–472, 1965.

Allègre, C., De l'extension de la méthode de calcul graphique Concordia aux mesures d'âges absolus effectués à l'aide du déséquilibre radioactif; Cas des minéralisations sécondaires d'uranium, *Compt. Rend., 259,* 4086–4089, 1964.

Allègre, C., and G. Michard, Sur les discordances des âges obtenus par les méthodes au strontium et à l'argon, *Compt. Rend., 259,* 4313–4316, 1964.

Catanzaro, E. J., and J. L. Kulp, Discordant zircons from the Little Belt (Montana), Beartooth (Montana) and Santa Catalina (Arizona) mountains, *Geochim. Cosmochim. Acta, 28,* 87–124, 1964.

Davis, G. L., G. R. Tilton, and G. W. Wetherill, Mineral ages from the Appalachian province in North Carolina and Tennessee, *J. Geophys. Res., 67,* 1987–1996, 1962.

Doe, B. R., and M. Newell, Isotopic composition of uranium in zircon, *Am. Mineralogist, 50,* 613–618, 1965.

Fleischer, R. L., P. B. Price, and R. M. Walker, Solid-state track detectors: Applications to nuclear science and geophysics, *Ann. Rev. Nuclear Sci., 15,* 1–28, 1965.

Gruenenfelder, M., Heterogenitaet akzessorischer Zirkone und die petrogenetische Deutung ihrer Uran/Blei-Zerfallsalter, 1, Der Zirkon des Granodioritgneises von Acquacalda (Lukmanierpass), *Schweiz. Min. Petr. Mitt., 43,* 235–257, 1963.

Hart, S. R., Current status of radioactive age determination methods, *Trans. Am. Geophys. Union, 47,* 280–286, 1966.

Holmes, A., The oldest dated minerals of the Rhodesian shield, *Nature, 173,* 612–614, 1954.

Holmes, A., and L. Cahen, African geochronology, Colonial Geology and Mineral Resources, *5,* 3–38, 1955.

Kelley, V. C., Geological map of the Sandia Mountains and vicinity, New Mexico, State Bureau of Mines and Mineral Resources, New Mexico Institute of Mining and Technology, Socorro, New Mexico, 1963.

Kovarik, A. F., and N. I. Adams, Jr., The disintegration constant of thorium and the branching ratio of thorium C, *Phys. Rev., 54,* 413–421, 1938.

Nicolaysen, L. O., Solid diffusion in radioactive minerals and the measurement of absolute age, *Geochim. Cosmochim. Acta, 11,* 41–59, 1957.

Senftle, F. E., T. A. Farley, and N. Lazar, Half-life of Th^{232} and the branching ratio of Bi^{212}, *Phys. Rev., 104,* 1629–1632, 1956.

Silver, L. T., The relation between radioactivity and discordance in zircons, *Nuclear Sci. Ser., Rept. 38, Natl. Acad. Sci. U. S. Publ. 1075,* pp. 34–42, 1962.

Silver, L. T., The use of cogenetic uranium-lead isotope systems in zircons in geochronology, in *Radioactive Dating,* pp. 279–287, International Atomic Energy Agency, Vienna, 1963.

Silver, L. T., and S. Deutsch, Uranium-lead methods on zircons, *Ann. N. Y. Acad. Sci., 91,* 279–283, 1961.

Silver L. T., and S. Deutsch, Uranium-lead isotopic variations in zircons: A case study, *J. Geol., 71,* 721–758, 1963.

Tilton, G. R., The interpretation of lead-age discrepancies by acid-washing experiments, *Trans. Am. Geophys. Union, 37,* 224–230, 1956.

Tilton, G. R., Volume diffusion as a mechanism for discordant lead ages, *J. Geophys. Res., 65,* 2933–2945, 1960.

Tilton, G. R., G. L. Davis, G. W. Wetherill, and L. T. Aldrich, Isotopic ages of zircon from granites and pegmatites, *Trans. Am. Geophys. Union, 38,* 360–371, 1957.

Tilton, G. R., and R. H. Steiger, Lead isotopes and the age of the earth, *Science, 150,* 1805–1808, 1965.

Tilton, G. R., G. W. Wetherill, and G. L. Davis, Mineral ages from the Wichita and Arbuckle Mountains, Oklahoma, and the St. Francis Mountains, Missouri, *J. Geophys. Res., 67,* 4011–4019, 1962.

Wasserburg, G. J., Diffusion processes in lead-uranium systems, *J. Geophys. Res., 68,* 4823–4846, 1963.

Wasserburg, G. J., D. Towell, and R. H. Steiger, A study of Rb-Sr systematics in some Precambrian granites of New Mexico (abstract), *Trans. Am. Geophys. Union 46,* 173–174, 1965.

Wetherill, G. W., Discordant uranium-lead ages, 1, *Trans. Am. Geophys. Union, 37,* 320–326, 1956.

Wetherill, G. W., Discordant uranium-lead ages, 2, Discordant ages resulting from diffusion of lead and uranium, *J. Geophys. Res., 68,* 2957–2965, 1963.

Wetherill, G. W., G. R. Tilton, G. L. Davis, S. R. Hart, and C. A. Hopson, Age measurements in the Maryland piedmont, *J. Geophys. Res., 71,* 2139–2155, 1966.

Whittaker, E. T., and G. N. Watson, *Modern Analysis,* Cambridge University Press, 1920.

(Received July 27, 1966;
revised September 13, 1966.)